





12

LEVEL II

6 INTERMEDIATE RESULTS OF THE RADAR BACKSCATTER STUDY OF SEA ICE IN THE BEAUFORT SEA.

10 C.V. Delker / R.G. Onstott / R.K. Moore, Principal Investigator

Remote Sensing Laboratory / Center for Research, Inc. / The University of Kansas / Lawrence, Kansas 66045

14 RSL Technical Report, RSL-TR-331-15

11 March 1980

Supported by:

OFFICE OF NAVAL RESEARCH / Department of the Navy / 800 N. Quincy Street / Arlington, Virginia 22217

CONTRACT/NO0014-76-C-1105 / 15

12 11

Accession For	
NTIS GRA&I	<input checked="" type="checkbox"/>
DDC TAB	<input checked="" type="checkbox"/>
Unannounced	<input type="checkbox"/>
Justification	
By Per Ltr. on file	
Distribution/	
Availability Codes	
Dist.	Avail and/or special
A	

DTIC ELECTE / APR 22 1980 / S D D

DISTRIBUTION STATEMENT A / Approved for public release; / Distribution Unlimited

ACKNOWLEDGEMENTS

The University of Kansas team of experimenters would especially like to express their thanks to Dr. René O. Ramseier, Ice Experiment Coordinator, for his cooperation and assistance throughout all phases of this measurement program.

We also wish to thank the Polar Continental Shelf Project for base camp privileges at Tuktoyaktuk and logistic support of our experimental efforts. We would especially like to acknowledge the assistance of Barry Hough, camp director.

We would like to acknowledge the expertise of Jim Hodges, pilot of the Okanagan Bell 205 helicopter, and Rich Tennant, engineer. Their valuable assistance in the successful completion of our program and their comic relief were most appreciated.

We also must acknowledge the cooperation we received from all the experimenters who worked at Tuktoyaktuk.

We would like to acknowledge the support of this research by the Office of Naval Research, Contract N00014-76-C-1105.

8-9' 1-4 (4-6' 1-2-6)

ABSTRACT

As a part of the Beaufort Sea segment of the Surveillance Satellite Project (SURSAT), a team of investigators from the University of Kansas conducted experiments to obtain quantitative measurements of radar backscatter from sea ice during the month of March 1979. Thick first-year sea ice, thin first-year sea ice, and an inland fresh water lake were studied using a surface-based FM-CW scatterometer that swept from 1.1 - 1.9 GHz and 8.5 - 17.5 GHz with angles of incidence (from vertical) of 10° to 75° and various linear polarizations. Measurements of thick first-year sea ice, thin first-year sea ice, brackish sea ice, and an inland fresh-water lake were also made using a helicopter-borne FM-CW scatterometer that swept from 8.5 - 17.5 GHz with incidence angles of 20° to 60° and VV polarization only.

8-9' 1-4

The 1.1 - 1.9 GHz measurements show that lake ice can be distinguished from thick and thin first-year sea ice. The radar cross-sections of thick and thin first-year sea ice are not significantly different for incidence angles less than 45°. The 8.5 - 17.5 GHz measurements indicate that lake ice can be distinguished from the other types in all cases. Thick and thin first-year sea ice are separated by a 2 - 4 dB difference for incidence angles greater than 40°. (See)

The effect of snow cover on the return from lake ice was also investigated with dramatic results. Returns from bare-surface lake ice were found to be 10 - 12 dB lower than the returns from snow-covered lake ice. This indicates that volume scatter in the snow may be the major contributor to lake ice backscatter when snow is present.

TABLE OF CONTENTS

	<u>Page</u>
ACKNOWLEDGEMENTS . . . . .	i
ABSTRACT . . . . .	ii
1.0 INTRODUCTION. . . . .	1
2.0 SYSTEM DESCRIPTION. . . . .	4
2.1 TRAMAS . . . . .	4
2.2 HELOSCAT . . . . .	8
3.0 TRAMAS RESULTS. . . . .	11
3.1 L-Band Results . . . . .	11
3.2 Ku-X-Band Results. . . . .	11
4.0 HELOSCAT RESULTS. . . . .	30
5.0 FREQUENCY RESPONSE. . . . .	35
6.0 CONCLUSIONS . . . . .	39
REFERENCES . . . . .	40

LIST OF TABLES

	<u>Page</u>
Table 1: SUMMARY OF BACKSCATTER MEASUREMENTS. . . . .	2
Table 2: NOMINAL SYSTEM SPECIFICATIONS (TRAMAS) . . . . .	6
Table 3: NOMINAL SYSTEM SPECIFICATIONS FOR HELI-BORNE SYSTEM (HELOSCAT). . . . .	9

LIST OF FIGURES

<u>Number</u>	<u>Figure Description</u>	<u>Page</u>
2.1	Block Diagram of HELOSCAT and TRAMAS System. . . . .	5
2.2	TRAMAS System in Operation at an Ice Site. . . . .	7
2.3	HELOSCAT System Installed on Bell 205 Helicopter . . . .	10
3.1	Average Scattering Coefficient of Thick First-Year, Thin First-Year, and Lake ice at 1.5 GHz (March 1979). . .	12
3.2	Average Scattering Coefficient of Thick First-Year and Thin First-Year Ice at 1.5 GHz (March 1979). . . . .	13
3.3	Average Scattering Coefficient of Thick First-Year, Thin First-Year, and Lake Ice at 9 GHz (March 1979). . .	14
3.4	Average Scattering Coefficient of Thick First-Year, Thin First-Year, and Lake Ice at 9 GHz (March 1979). . .	15
3.5	Average Scattering Coefficient of Thick First-Year, Thin First-Year, and Lake Ice at 9 GHz (March 1979). . .	16
3.6	Average Scattering Coefficient of Thick First-Year, Thin First-Year, and Lake Ice at 13 GHz (March 1979) . .	17
3.7	Average Scattering Coefficient of Thick First-Year, Thin First-Year, and Lake Ice at 13 GHz (March 1979) . .	18
3.8	Average Scattering Coefficient of Thick First-Year, Thin First-Year, and Lake Ice at 13 GHz (March 1979) . .	19
3.9	Average Scattering Coefficient of Thick First-Year, Thin First-Year, and Lake Ice at 17 GHz (March 1979) . .	20
3.10	Average Scattering Coefficient of Thick First-Year, Thin First-Year, and Lake Ice at 17 GHz (march 1979) . .	21
3.11	Average Scattering Coefficient of Thick First-Year, Thin First-Year, and Lake Ice at 17 GHz (March 1979) . .	22
3.12	Scattering Coefficient of Lake Ice with Bare, Normal, Rough, and Very Rough Snow Cover Conditions at 9 GHz (March 1979) . . . . .	25
3.13	Scattering Coefficient of Lake Ice with Bare, Normal, Rough, and Very Rough Snow Cover Conditions at 9 GHz (March 1979) . . . . .	26

LIST OF FIGURES (continued)

<u>Number</u>	<u>Figure Description</u>	<u>Page</u>
3.14	Scattering Coefficient of Lake Ice with Bare, Normal, Rough, and Very Rough Snow Cover at 17 GHz (March 1979) . . . . .	27
3.15	Scattering Coefficient of Lake Ice with Bare, Normal, Rough, and Very Rough Snow Cover Conditions at 17 GHz (March 1979) . . . . .	28
3.16	Difference Between Radar Cross-Section of Thin First-Year and Thick First-Year Sea Ice at 1.5, 9.0, 13.0, and 17.0 GHz with Vertical Polarization (TRAMAS, March 1979). . . . .	29
3.17	Difference Between Radar Cross-Section of Thick First-Year Sea Ice and Lake Ice at 1.5, 9.0, 13.0 and 17.0 GHz with Vertical Polarization (TRAMAS, March 1979). . .	29
4.1	Average Scattering Coefficient of Thick First-Year, Thin First-Year, Brackish, and Lake Ice at 9 GHz (March 1979) . . . . .	31
4.2	Average Scattering Coefficient of Thick First-Year, Thin First-Year, Brackish, and Lake Ice at 13 GHz (March 1979) . . . . .	32
4.3	Average Scattering Coefficient of Thick First-Year, Thin First-Year, Brackish, and Lake ice at 17 GHz (March 1979) . . . . .	33
4.4	Difference Between Radar Cross-Section of Thin First-Year and Thick First-Year Sea Ice at 9.0, 13.0, and 17.0 GHz with Vertical Polarization (HELOSCAT, March 1979). . . . .	34
4.5	Difference Between Radar Cross-Section of Thick First-Year and Lake Ice at 9.0, 13.0, and 17.0 GHz with Vertical Polarization (HELOSCAT, march 1979). . . . .	34
5.1	Scattering Coefficient Frequency Response of Thick First-Year, Thin First-Year, and Lake Ice (March 1979) . . . .	36
5.2	Scattering Coefficient Frequency Response of Thick First-Year, Thin First-Year, Brackish, and Lake Ice (March 1979) . . . . .	37

## 1.0 INTRODUCTION

During the month of March 1979, a research team from the University of Kansas Remote Sensing Laboratories conducted experiments designed to investigate the radar backscatter properties of sea ice. This investigation was a part of the Beaufort Sea segment of the Surveillance Satellite Project (SURSAT) which occurred off the Canadian coast near Tuktoyaktuk, N.W.T., Canada. The Polar Continental Shelf Project facilities located at Tuktoyaktuk served as a base of operations for these experiments.

The experiments performed by the K.U. team may be divided into two parts. Part one utilized the surface-based Transportable Microwave Active Spectrometer (TRAMAS) system [1,2]. Measurements of thick first-year sea ice, thin first-year sea ice, and an inland fresh water lake were obtained during this portion of the experiment. Part two of the experiment utilized the helicopter-borne scatterometer (HELOSCAT) system [3]. Backscatter measurements from thick first-year sea ice, thin first-year sea ice, brackish sea ice, and the inland fresh-water lake were obtained with this system. A summary of the measurements obtained with each system is presented in Table 1.

The L-band measurements obtained with the TRAMAS system indicate that it is possible to distinguish lake ice from thick and thin first-year sea ice at all incidence angles for this frequency. Thick and thin first-year sea ice are separated by 1-2 dB for incidence angles greater than  $45^\circ$ . The results of the Ku-X-band measurements from both the TRAMAS and HELOSCAT systems indicate that lake ice can be distinguished from the other types in all cases. The TRAMAS results indicate that thick and thin first-year sea ice are separated by 2-4 dB for incidence angles greater than  $40^\circ$  while

TABLE 1  
SUMMARY OF BACKSCATTER MEASUREMENTS

Sensor	Date	Site Number	Ice Type	Number of Looks
TRAMAS	3/13	T1	Lake	2
	3/14	T2	TFY	3
	3/15	T3	TFY	4
	3/16	T4	Young	3
	3/21	T5	Lake	5
HELOSCAT	3/31	H1	Lake	10
	4/1	H2	Lake	10
	4/1	H3	Brackish	13
	4/1	H4	TFY	10
	4/1	H5	TFY	10
	4/1	H6	TFY	10
	4/1	H7	Young	15
	4/1	H8	Brackish	14

the HELOSCAT results show a 2-6 dB difference. The brackish sea ice observed with the HELOSCAT system resulted in trends that were very similar to those obtained from thick first-year sea ice.

An experiment that was done to determine the effects of snow on the backscatter return from lake ice provided some dramatic results. The return from the bare lake-ice surface was found to be 10-12 dB lower than the returns from snow-covered lake ice. This would seem to indicate that volume scatter from the snow may be the major contributor to backscatter from lake ice when snow is present on the surface.

## 2.0 SYSTEM DESCRIPTION

Measurements of radar backscatter from sea ice were obtained using two systems -- the surface-based TRAMAS system and the helicopter-mounted version, HELOSCAT. Both systems are frequency-modulated continuous-wave (FM-CW) scatterometers. A system block diagram is shown in Figure 2.1. Only the Ku-X-Band antennas and electronics are used in the HELOSCAT system.

### 2.1 TRAMAS

The Transportable Microwave Active Spectrometer (TRAMAS) system is a four antenna FM-CW scatterometer mounted on a portable surface-based structure. The L-band radar is swept from 1.1 to 1.9 GHz for VV and VH polarizations (H = horizontal, V = vertical; the first letter identifies transmitted polarization and the second identifies received polarization). The Ku-X-Band radar is swept from 8.5 to 17.5 GHz with HH, HV, VH, and VV polarizations. These radars operate at a fixed range from the ice surface with selectable angles of incidence of 10° to 75°. Table 2 details nominal system specifications for both radars and Figure 2.2 shows the assembled system during operation.

Calibration of the scatterometer is achieved by frequently passing the signal through a delay line of known attenuation and by less frequently observing a standard radar target of known cross-section.

This system was designed to be disassembled and moved from site to site using a small aircraft, helicopter, or snowmobile and sled. A Bell model 206 helicopter provided for experiment and program support by the Canadian Polar Continental Shelf Project (P.C.S.P.) was used to sling the structure from site to site during this experiment.

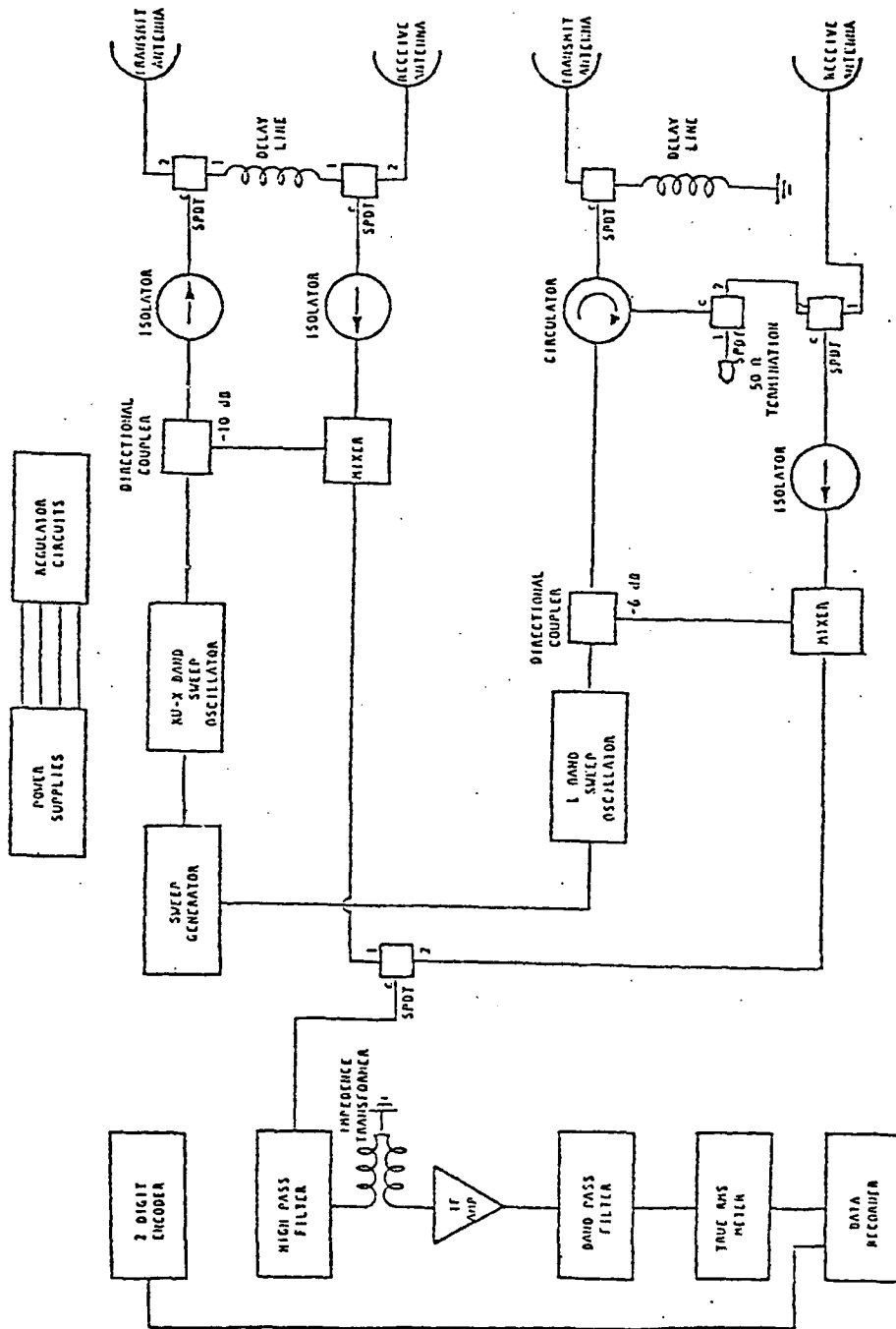


FIGURE 2.1  
Block Diagram of HELOSCAT and TRAMAS System

TABLE 2  
 NOMINAL SYSTEM SPECIFICATIONS (TRAMAS)

	<u>Ku-X-Band</u>	<u>L-Band</u>
Type	FM-CW	FM-CW
Frequency Range	8-18 GHz	1.5 GHz
Modulating Waveform	Triangular	Triangular
FM Sweep: $\Delta f$	1 GHz	800 MHz
Transmitter Power	14-19 dBm	19 dBm
Intermediate Frequency	50 kHz	50 kHz
IF Bandwidth	13.5 kHz	13.5 kHz
Antennas		
Receive Type	46 cm. Reflector	91 cm. Reflector
Transmit Type	31 cm. Reflector	Standard Gain Horn
Feeds	Dual Ridge Horn	Log Periodic
Polarization Capabilities	HH,HV,VV,VH	VV,VH
Target Distance	10.9 meters	6.5 meters
Transmit Beamwidth	8.2 <sup>0</sup> at 8 GHz 4.0 <sup>0</sup> at 17.7 GHz	27 <sup>0</sup>
Receive Beamwidth	5.3 <sup>0</sup> at 8 GHz 2.3 <sup>0</sup> at 17.8 GHz	9.5 <sup>0</sup>
Incidence Angle Range	10 <sup>0</sup> -75 <sup>0</sup>	10 <sup>0</sup> -75 <sup>0</sup>
Calibration:		
Internal	Signal Injection (delay line)	Signal Injection (shorted delay line)
External	Luneberg Lens Reflector	Luneberg Lens Reflector
Operating Temperature Range	-50 <sup>0</sup> C to +50 <sup>0</sup> C	-50 <sup>0</sup> C to +50 <sup>0</sup> C

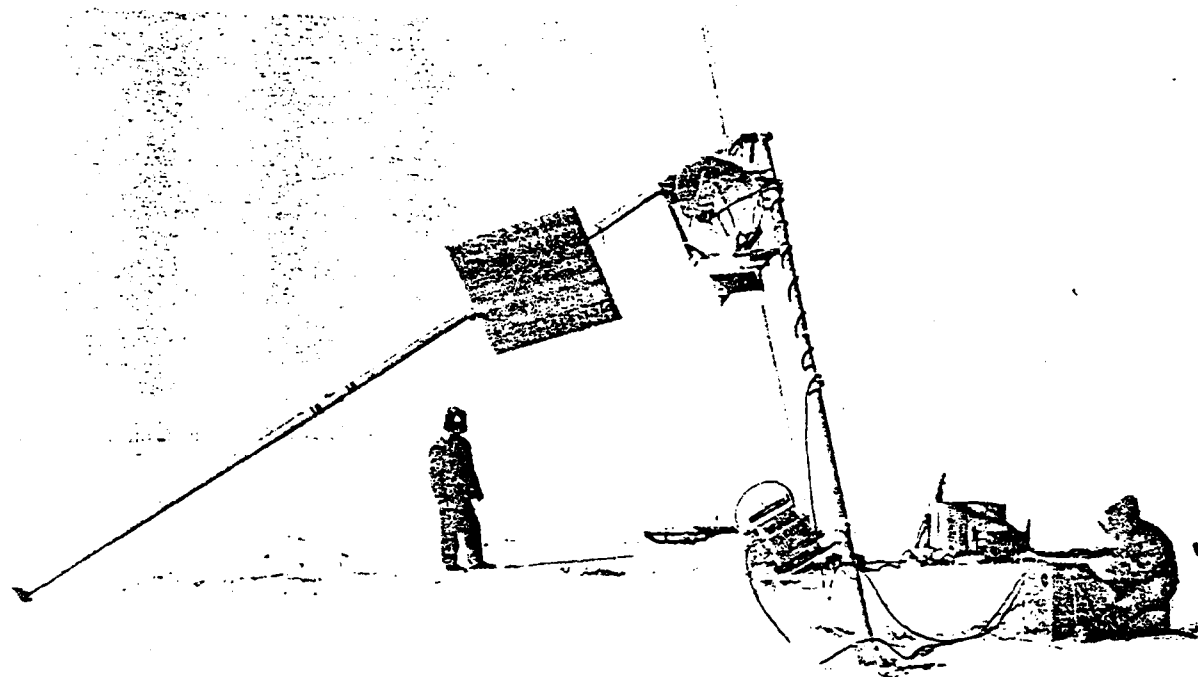


FIGURE 2.2

TRAMAS System in Operation at an Ice Site

## 2.2 HELOSCAT

The HELOSCAT system is a two antenna Ku-X-Band FM-CW scatterometer mounted on a Bell model 205 helicopter. This is the same radar as used with the TRAMAS system, but it is limited to VV polarization and 20°, 40° and 60° angles of incidence. Table 3 details the system specifications and Figure 2.3 shows the antennas and structure mounted on the helicopter. The HELOSCAT system also incorporates a radar altimeter to provide accurate information about altitude during the data acquisition. Calibration procedures are the same as those used for the TRAMAS system.

TABLE 3

NOMINAL SYSTEM SPECIFICATIONS FOR HELI-BORNE SYSTEM (HELOSCAT)

	<u>Ku-X-Band</u>
Type	FM-CW
Frequency Range	8-18 GHz
Modulating Waveform	Triangular
FM Sweep: $\Delta f$	1.0 GHz
Transmitter Power	14-19 dBm
Intermediate Frequency	50 kHz
IF Filter Bandwidth	13.5 kHz
Antennas	
Receive Type	46 cm. Reflector
Transmit Type	31 cm. Reflector
Feeds	Dual Ridge Horn
Polarization Capabilities	VV
Transmit Beamwidth	8.2 <sup>0</sup> at 8.0 GHz 4.0 <sup>0</sup> at 17.7 GHz
Receive Beamwidth	5.3 <sup>0</sup> at 8.0 GHz 2.3 <sup>0</sup> at 17.8 GHz
Incidence Angles Available	20 <sup>0</sup> , 40 <sup>0</sup> , and 60 <sup>0</sup>
Calibration:	
Internal	Signal Injection (delay line)
External	Luneberg Lens Reflector
Operating Temperature Range	-50 <sup>0</sup> C to +50 <sup>0</sup> C

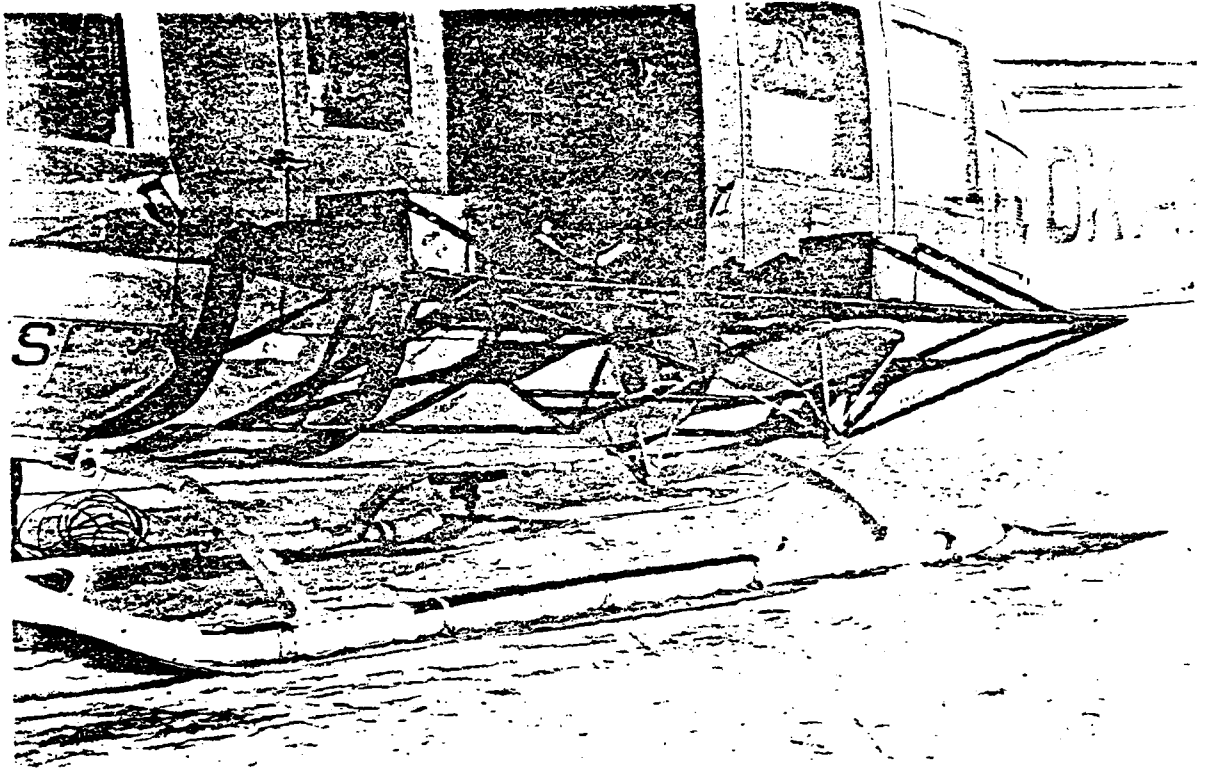


FIGURE 2.3

HELOSCAT System Installed on Bell 205 Helicopter

### 3.0 TRAMAS RESULTS

During the TRAMAS phase of the experiment three different types of ice were investigated. Included were fresh-water lake ice, thick first-year sea ice, and thin first-year sea ice. The lake was located a short distance from the P.C.S.P. buildings and was frozen to the bottom. It served as a convenient location for the initial setup and testing of the equipment before moving offshore to the pack ice sites. The thick first-year sea ice investigations were conducted on an undeformed expanse of ice designated as Site A by the experimenters. The thin first-year sea ice was located a few miles to the north of Site A on a refrozen lead.

#### 3.1 L-Band Results

The average scattering coefficients obtained with the L-Band radar are shown on the graphs of Figures 3.1 and 3.2. These graphs indicate that it is possible to discriminate between lake ice and thick or thin first-year sea ice with VV polarization, particularly for angles of incidence between  $20^\circ$  and  $60^\circ$ . No lake-ice data were available for VH polarization at this frequency. Thick and thin first-year sea ice are very similar for VV polarization with thin slightly below thick at incidence angles greater than  $40^\circ$ . Cross-polarization (VH) provides good discrimination of thin and thick first-year sea ice (3-4 dB) for incidence angles greater than  $40^\circ$ .

#### 3.2 Ku-X-Band Results

Scattering coefficient trends of thick first-year sea ice, thin first-year sea ice, and freshwater lake ice at 9, 13, and 17 GHz are shown in Figures 3.3 through 3.11. Discrimination between these three ice types may be possible for all frequencies in the 8-18 GHz region with the

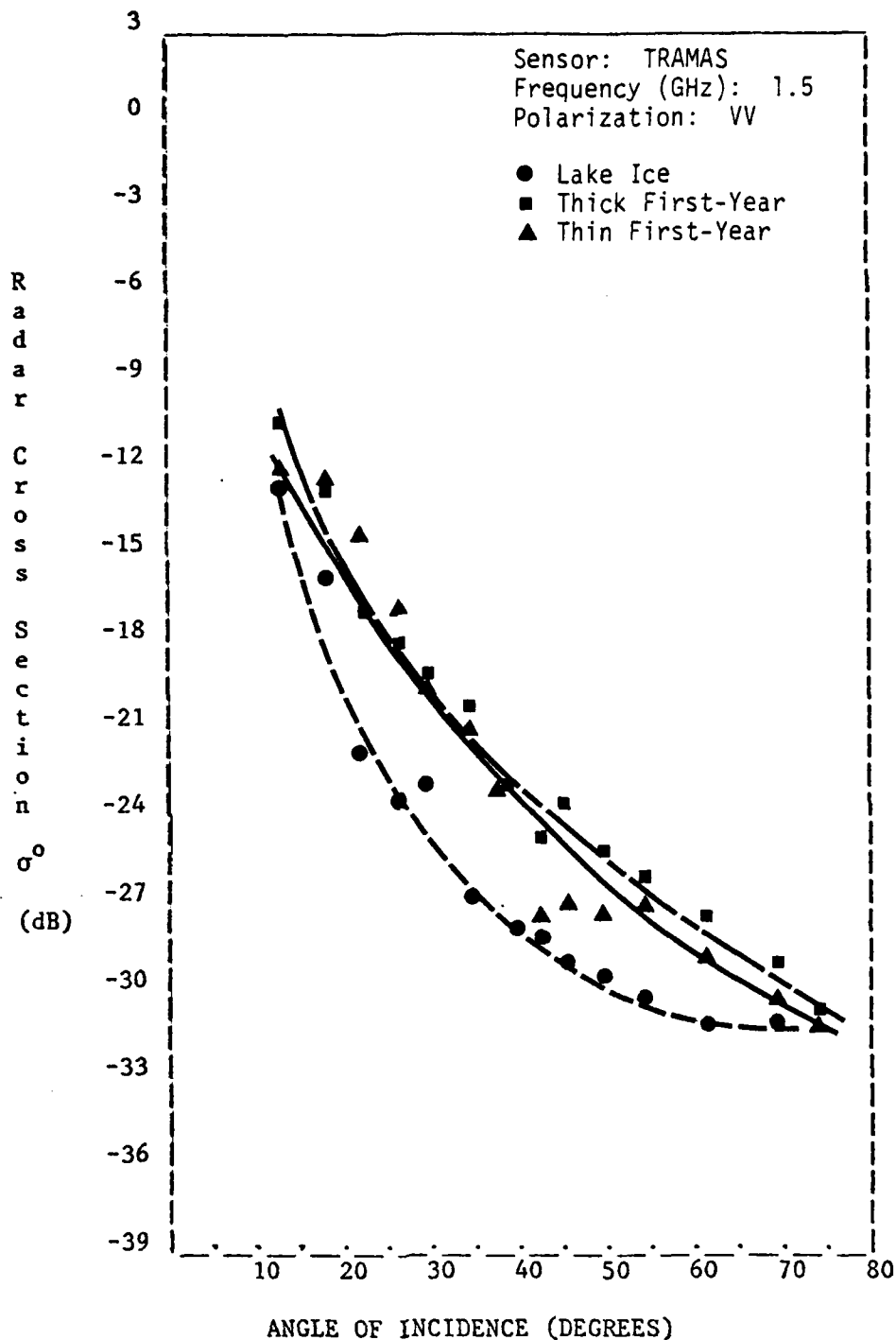


Figure 3.1. Average scattering coefficient of Thick First-Year, Thin First-Year, and Lake Ice at 1.5 GHz. (March 1979)

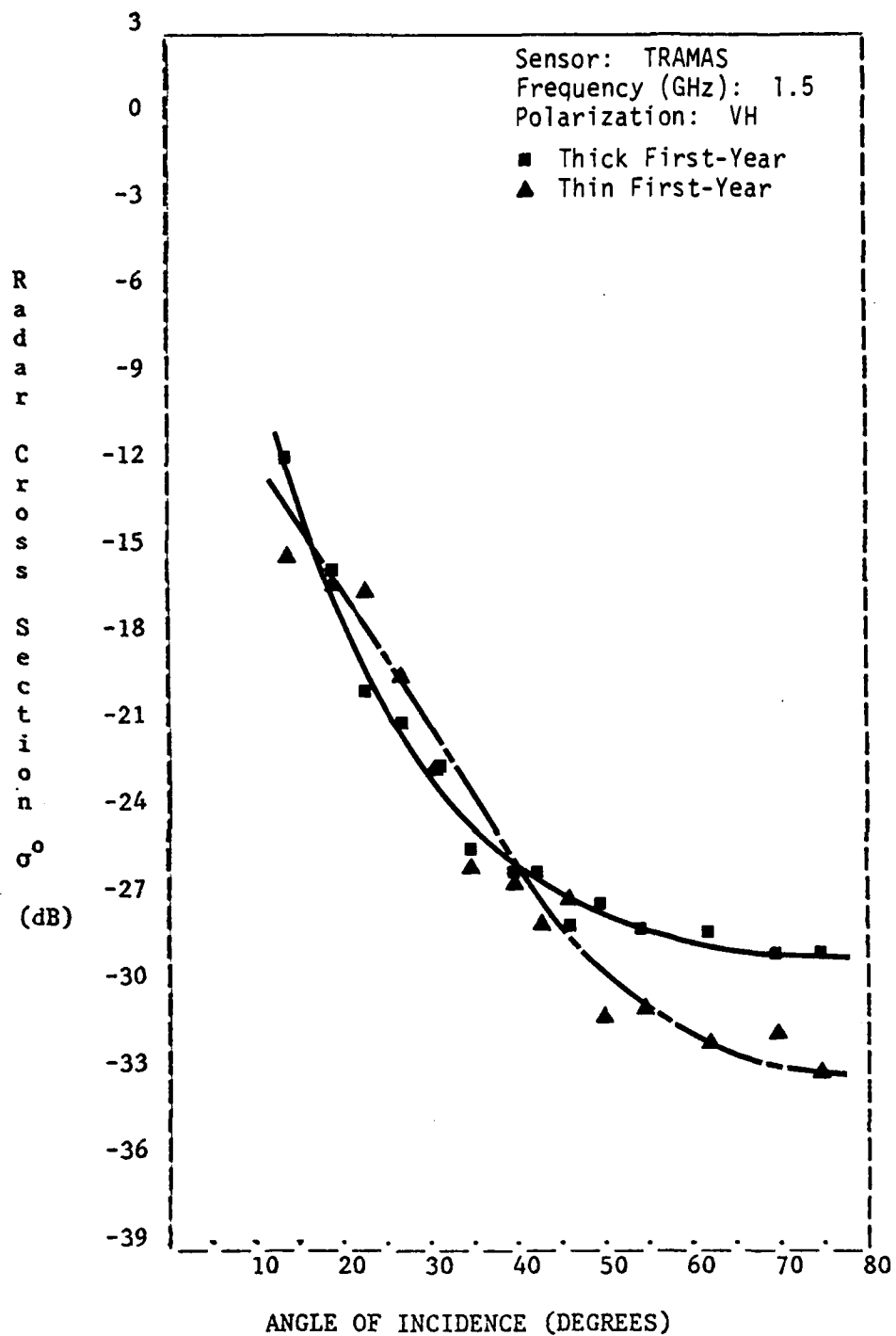


Figure 3.2. Average scattering coefficient of Thick First-Year and Thin First-Year Ice at 1.5 GHz. (March 1979)

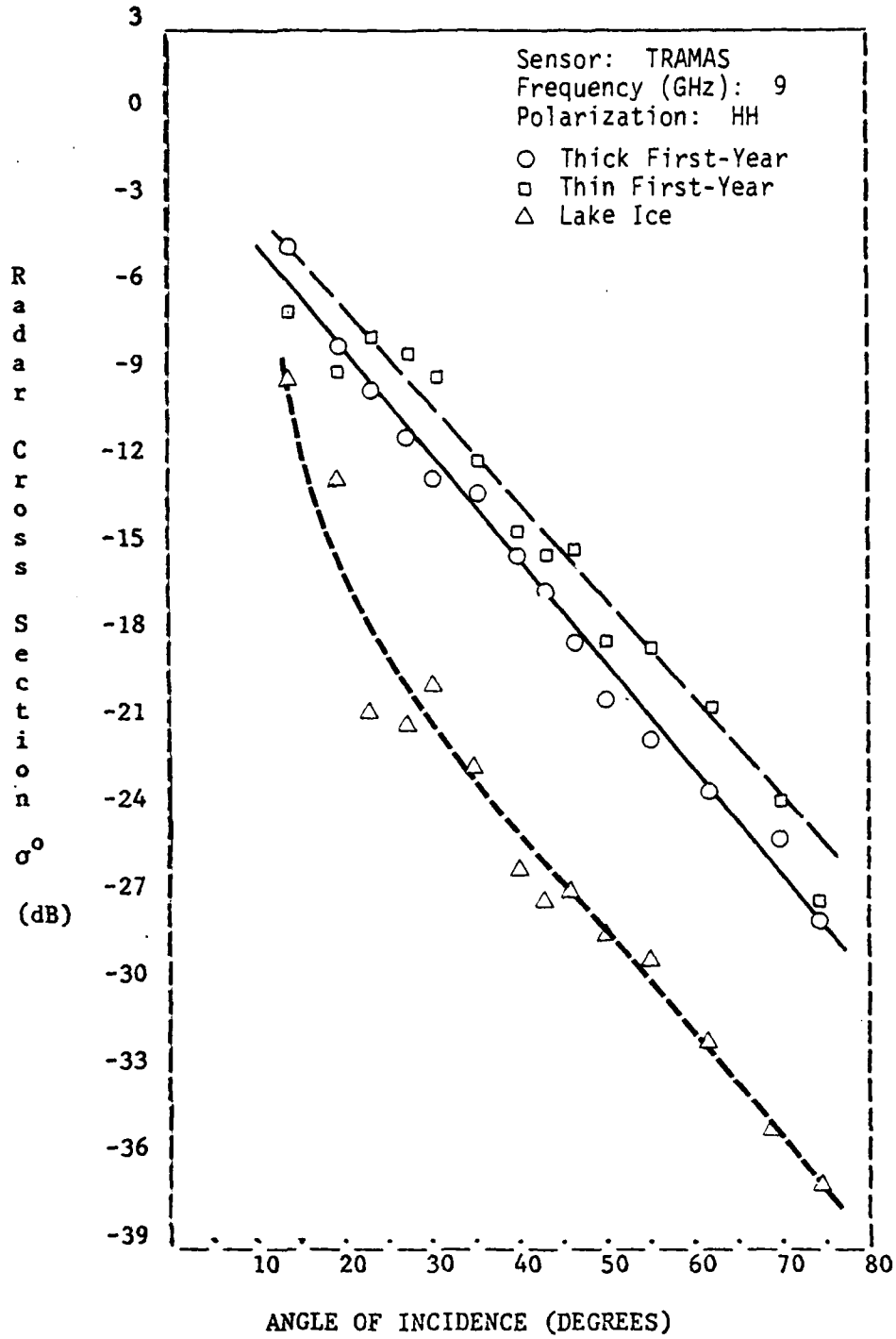


Figure 3.3. Average scattering coefficient of Thick First-Year, Thin First-Year, and Lake Ice at 9 GHz. (March 1979)

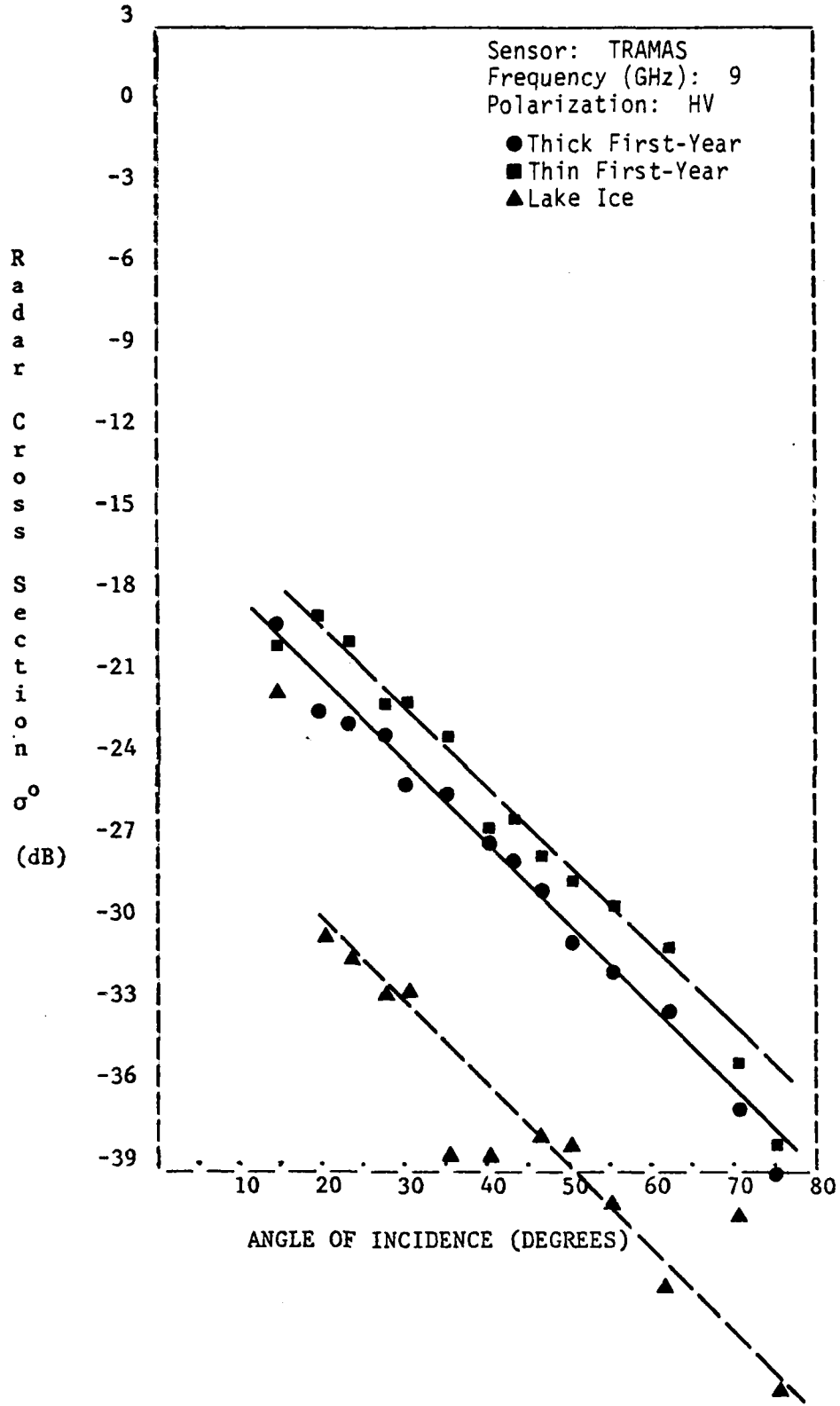


Figure 3.4. Average scattering coefficient of Thick First-Year, Thin First-Year, and Lake Ice at 9 GHz. (March 1979)

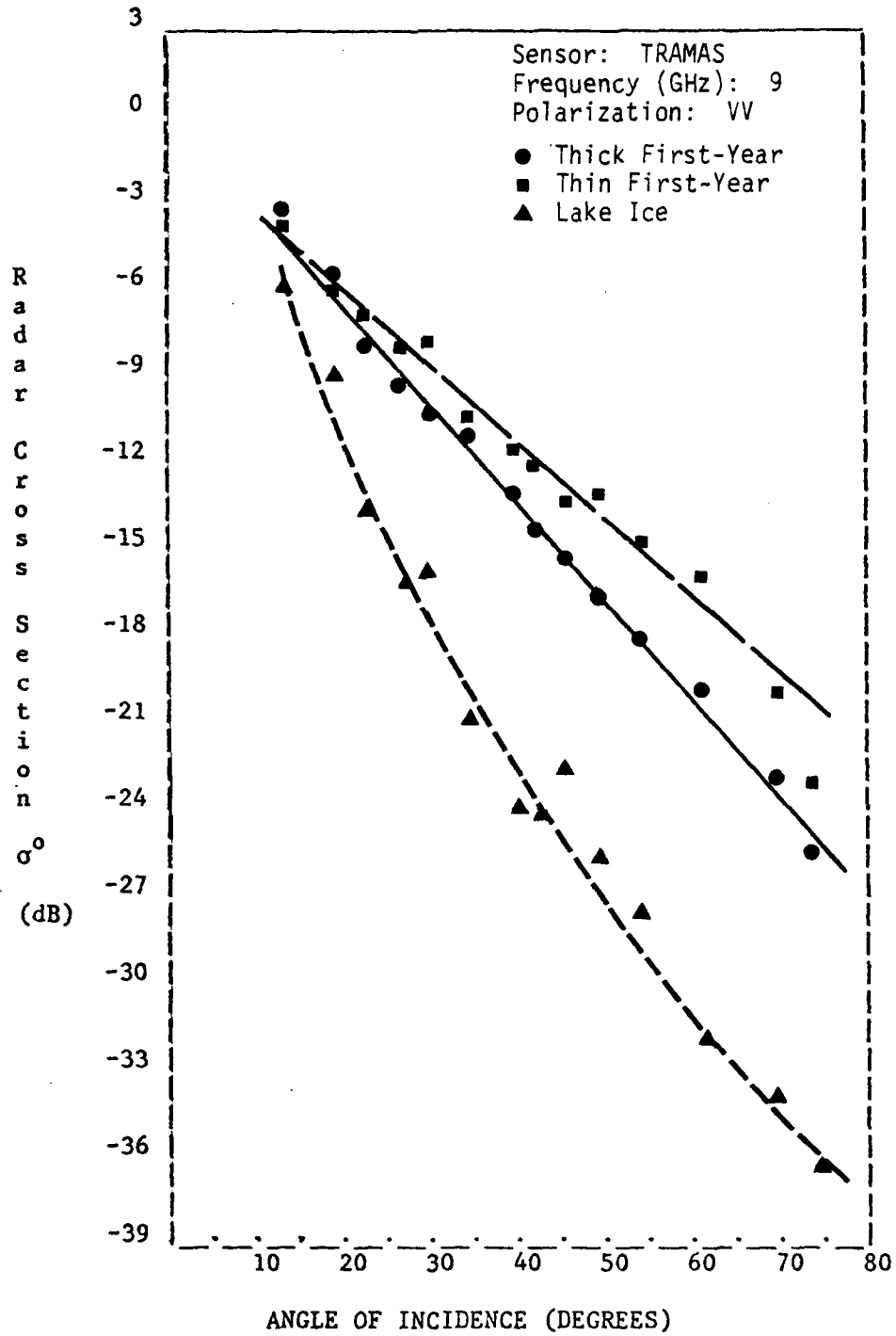


Figure 3.5. Average scattering coefficient of Thick First-Year, Thin First-Year, and Lake Ice at 9 GHz. (March 1979)

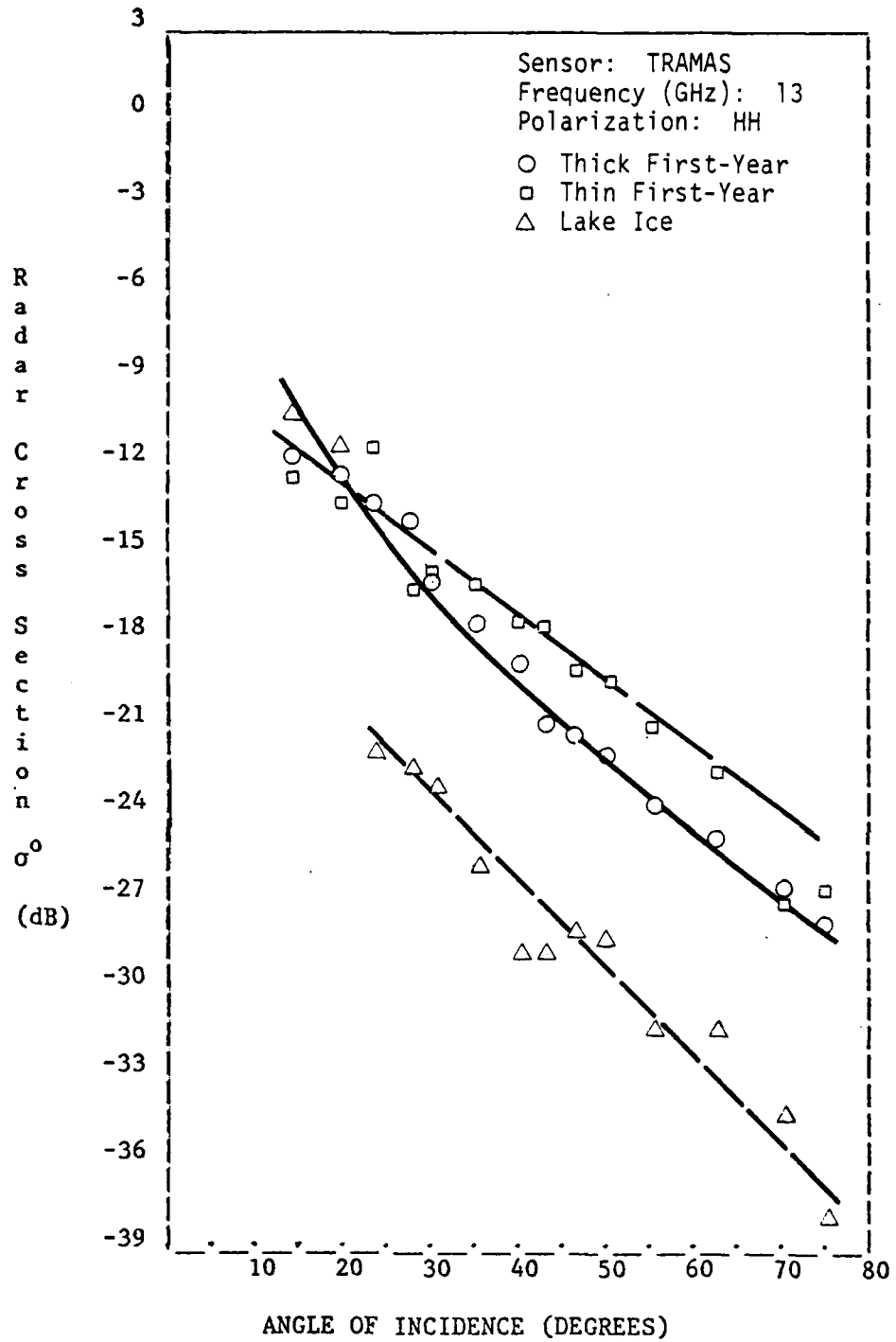


Figure 3.6. Average scattering coefficient of Thick First-Year, Thin First-Year, and Lake Ice at 13 GHz. (March 1979)

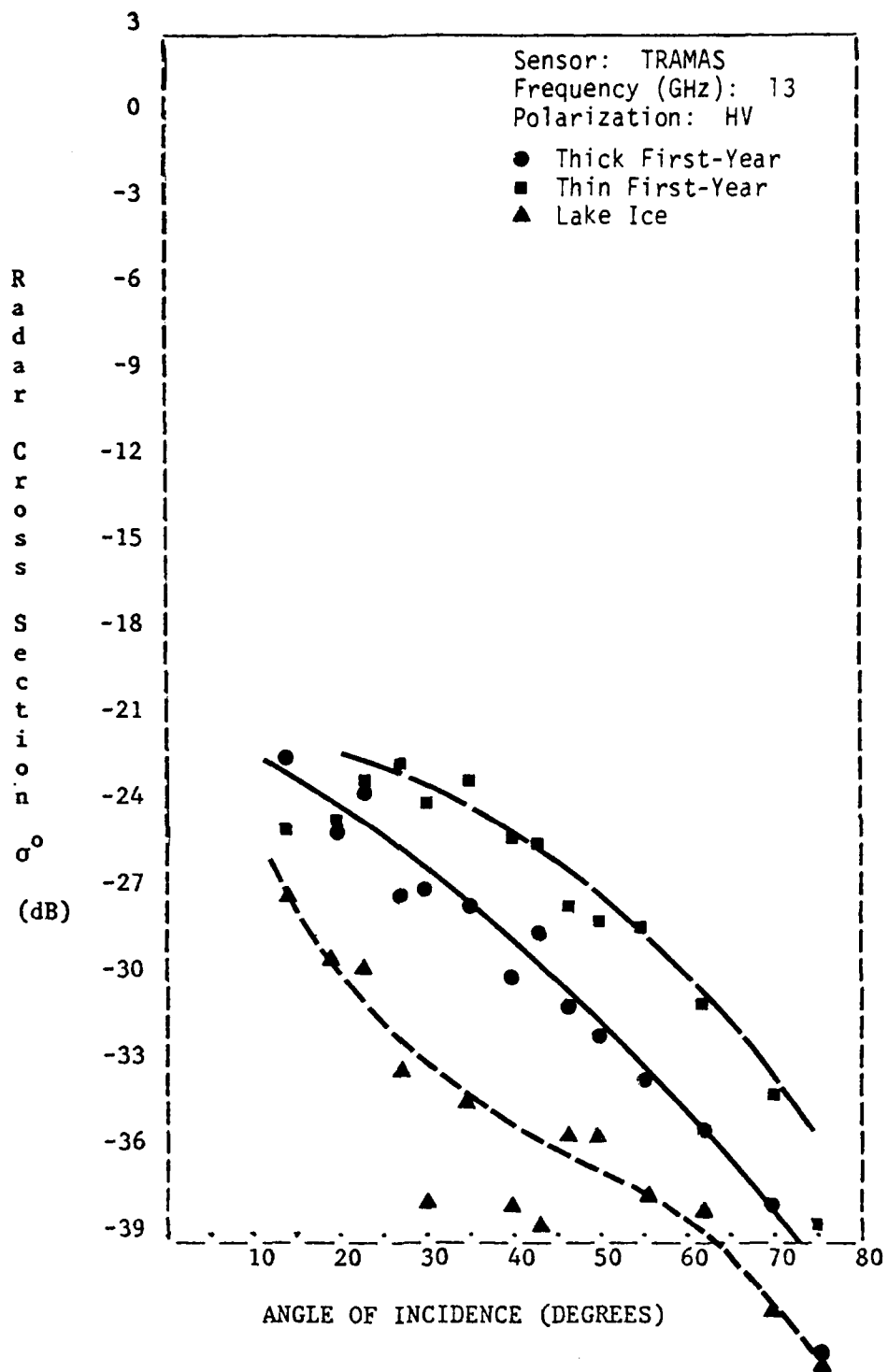


Figure 3.7. Average scattering coefficient of Thick First-Year, Thin First-Year, and Lake Ice at 13 GHz. (March 1979)

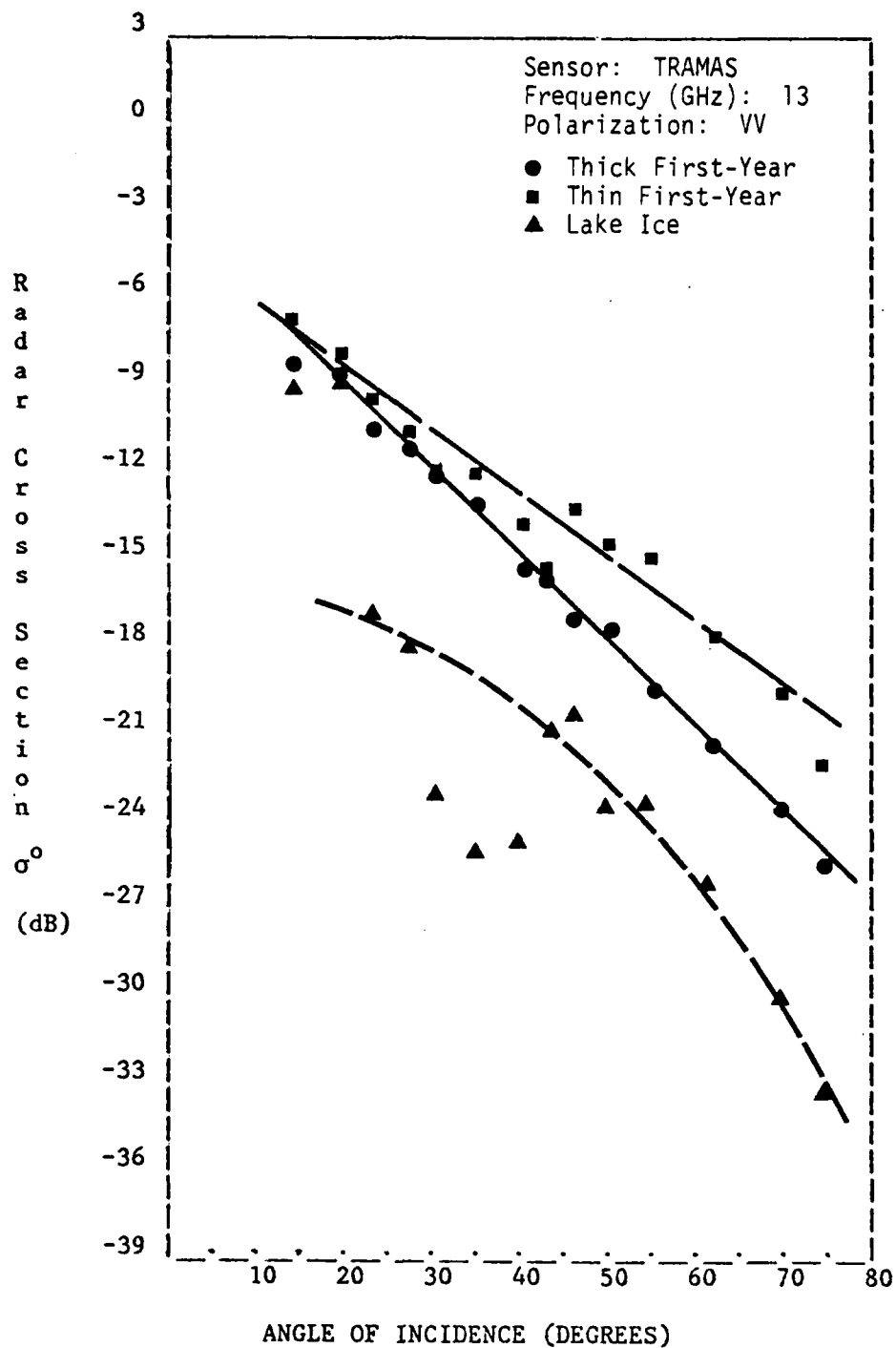


Figure 3.8. Average scattering coefficient of Thick First-Year, Thin First-Year, and Lake Ice at 13 GHz. (March 1979)

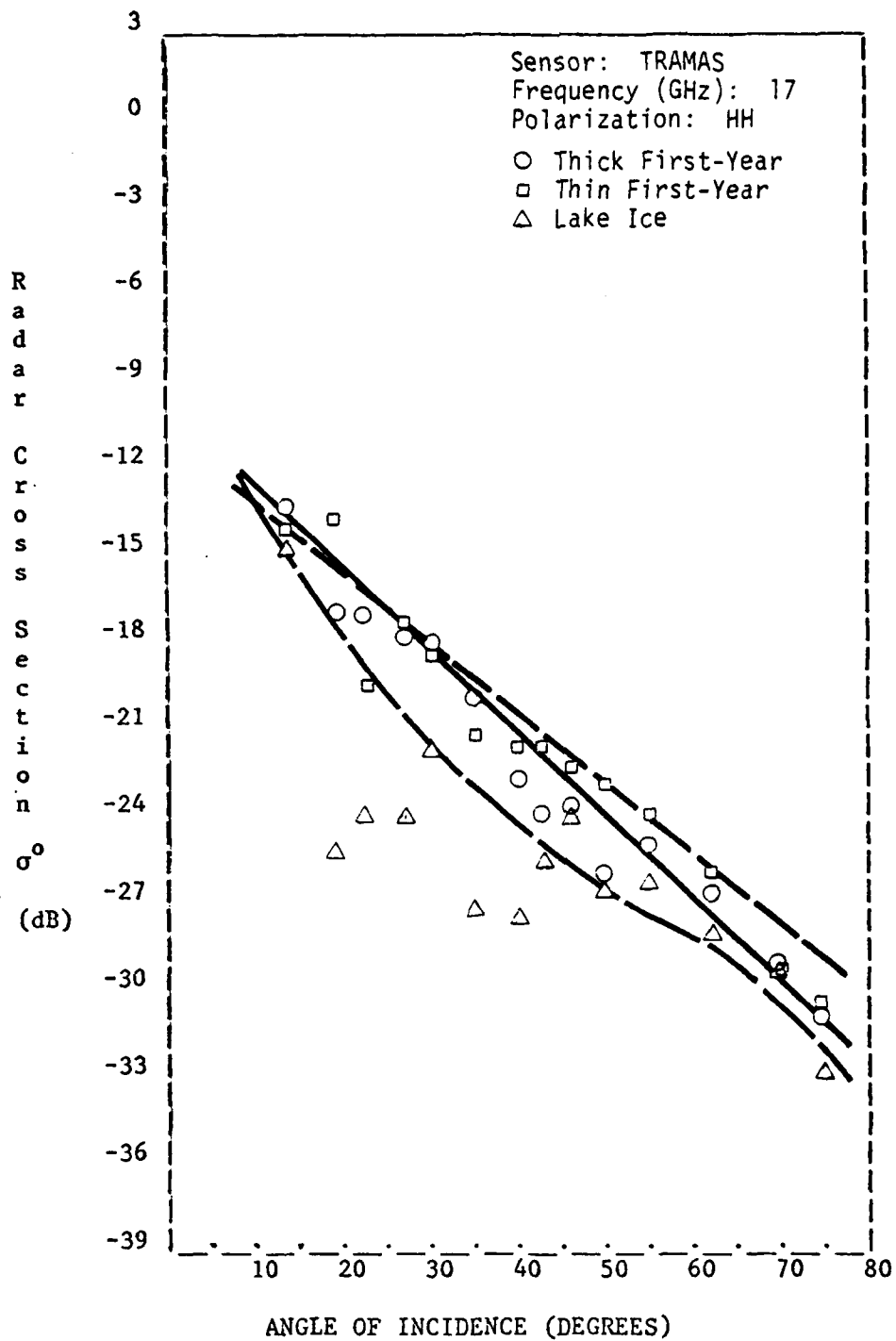


Figure 3.9. Average scattering coefficient of Thick First-Year, Thin First-Year, and Lake Ice at 17 GHz. (March 1979)

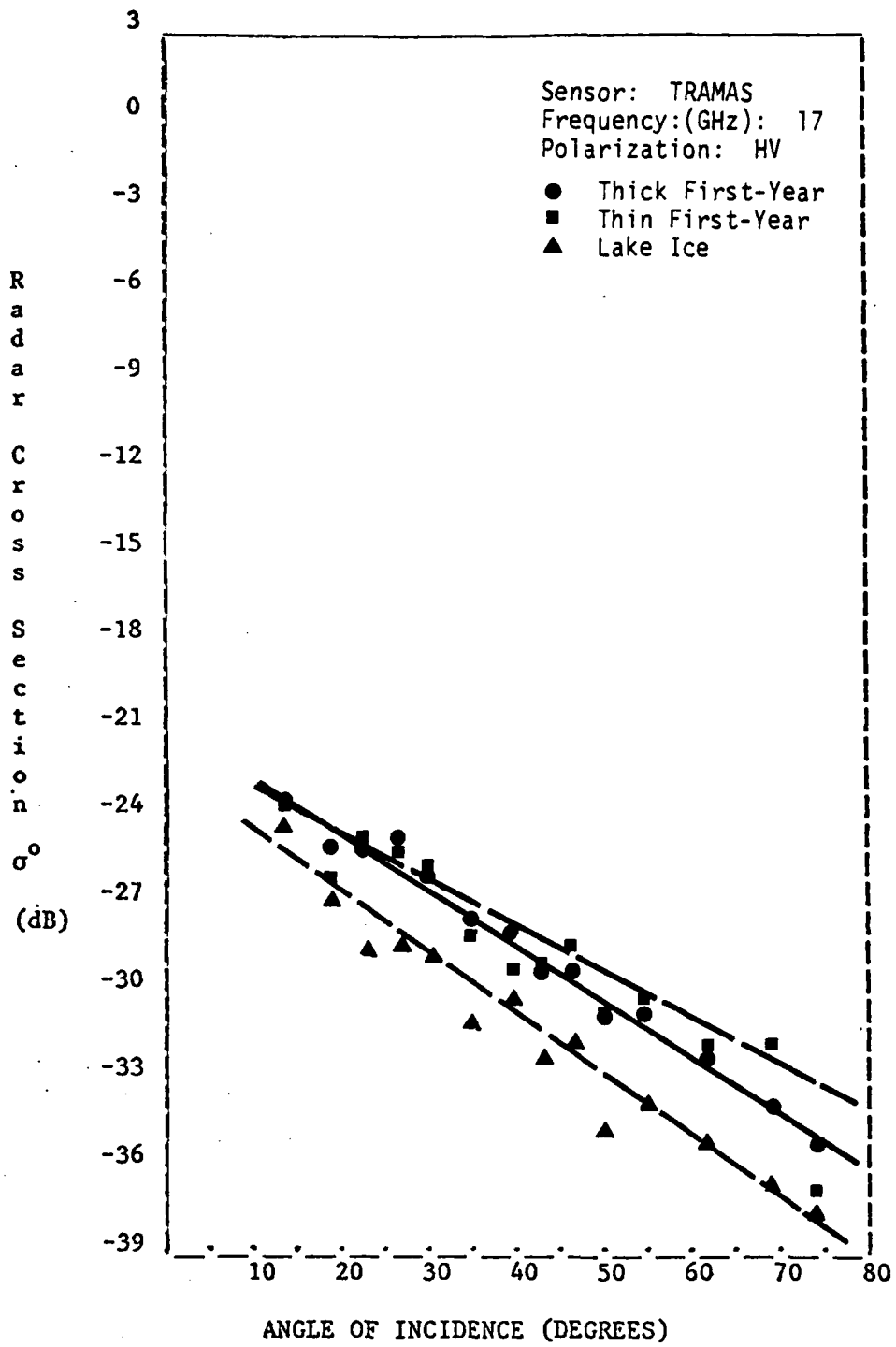


Figure 3.10. Average scattering coefficient of Thick First-Year, Thin First-Year, and Lake Ice at 17 GHz. (March 1979)

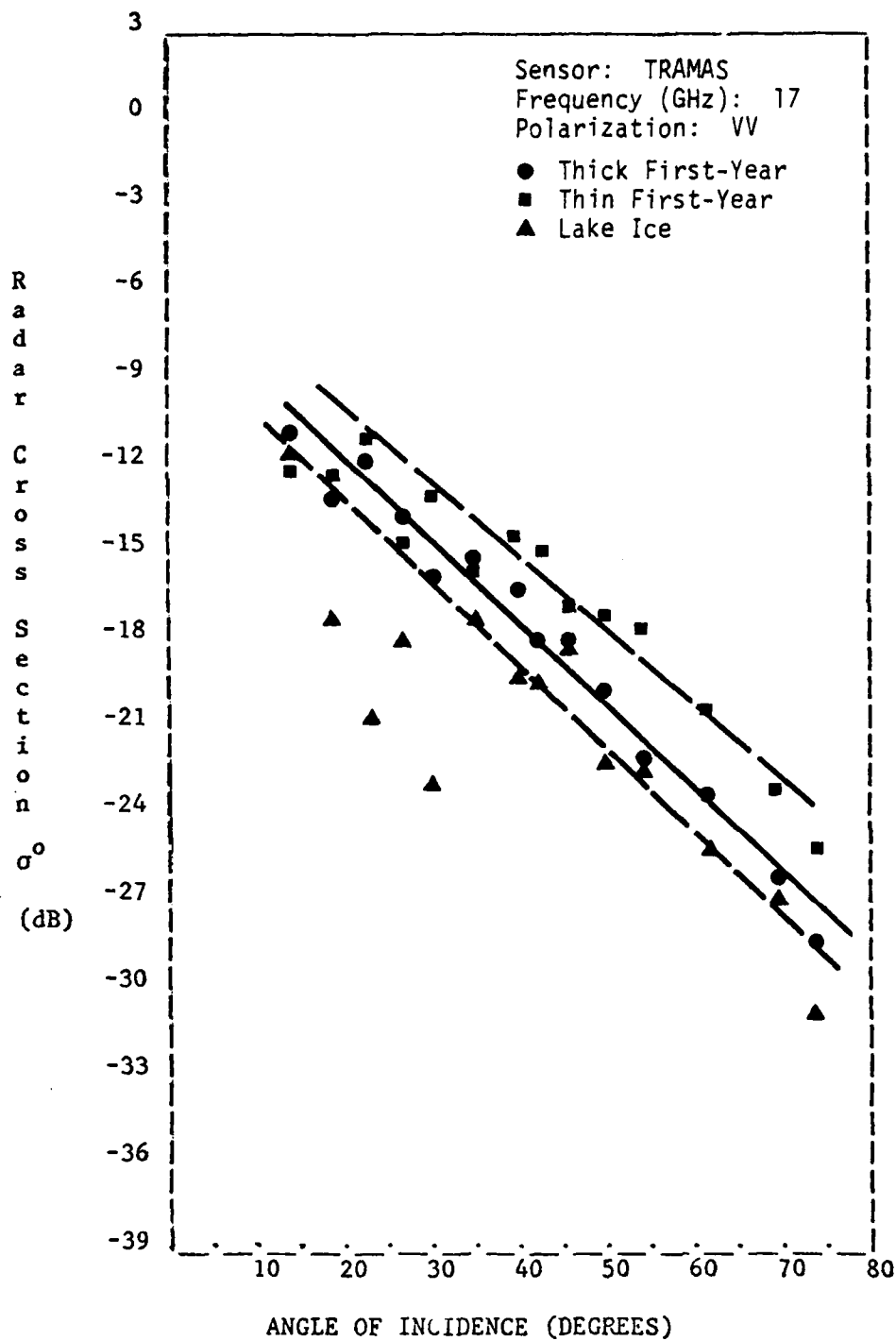


Figure 3.11. Average scattering coefficient of Thick First-Year, Thin First-Year, and Lake Ice at 17 GHz. (March 1979)

selection of the proper incidence angle. In each case lake ice had the lowest backscatter return and can easily be discriminated from the two first-year sea ice types. The thick and thin sea ice scattering coefficients demonstrate parallel angular response trends in most of the cases. The greatest separation occurs for large incidence angles at 9 GHz and vertical polarization. This is also the case for the difference between thick first-year sea ice and lake ice (see Figures 3.16 and 3.17). As the frequency increases the separation between returns from different ice types decreases. This indicates that a radar operating at 9 GHz with a large incidence angle would produce the best discrimination.

It is interesting to note the relation between the salinity of the ice type and the magnitude of the scattering coefficients for each type. Thin first-year sea ice, which has the highest salinity, also produced the highest scattering coefficient; while lake ice, which has a very low salinity, produced the lowest scattering coefficient. Thick first-year sea ice is located between the two in both respects. This observation is also true for the HELOSCAT data which will be discussed in the next section. The brackish ice investigated during that portion of the experiment produced coefficients slightly lower than those for thick first-year ice, corresponding to its lower salinity.

During the lake-ice portion of the experiment a set of measurements was made to study the effects of snow cover on the backscatter coefficient. Initial measurements were made without the snow cover being disturbed by the experimenters. Old snowmobile tracks and small surface features caused by the wind were characteristic of this hard-packed snow cover. In contrast to this natural 4 cm snow cover, the surface was artificially roughened with grooves 4 cm deep and 3 cm wide spaced 6 inches apart in a grid fashion. The snow was then completely removed from the target area.

The results of this process are illustrated in Figures 3.12 through 3.15. The horizontally polarized scatter was affected more by the roughening than the vertically polarized scatter. The orientation of the horizontal component of the radar signal with the grooves may be responsible for this dominant backscatter feature for HH polarization. The angular responses at vertical polarization for the natural and roughened cases were similar.

In all cases the scattering coefficient for the bare-surface lake ice was dramatically lower than the snow-covered-lake responses. The difference averaged 8 dB or greater. These results indicate that even at these very cold temperatures snow plays a very important role in the backscatter from lake ice and that this must be taken into account when extracting information from imagery of frozen lakes. Snow surface roughness also has been shown to have an effect on backscatter and should be accounted for.

The difference between thick first-year and thin first-year sea ice and between thick first-year sea ice and lake ice is plotted versus angle of incidence for 1.5, 9, 13, and 17 GHz in Figures 3.16 and 3.17. There is little ability to discriminate thick from thin ice with 1.5 GHz. All of the other frequencies indicate similar ability to discriminate between thick and thin first-year sea ice with the greatest difference occurring for angles of incidence greater than 40°. Figure 3.17 shows that all of the frequencies have the ability to discriminate thick first-year sea ice from lake ice for almost all angles of incidence. The 9.0 GHz frequency has a significantly larger difference (2-4 dB) for incidence angles greater than 40°.

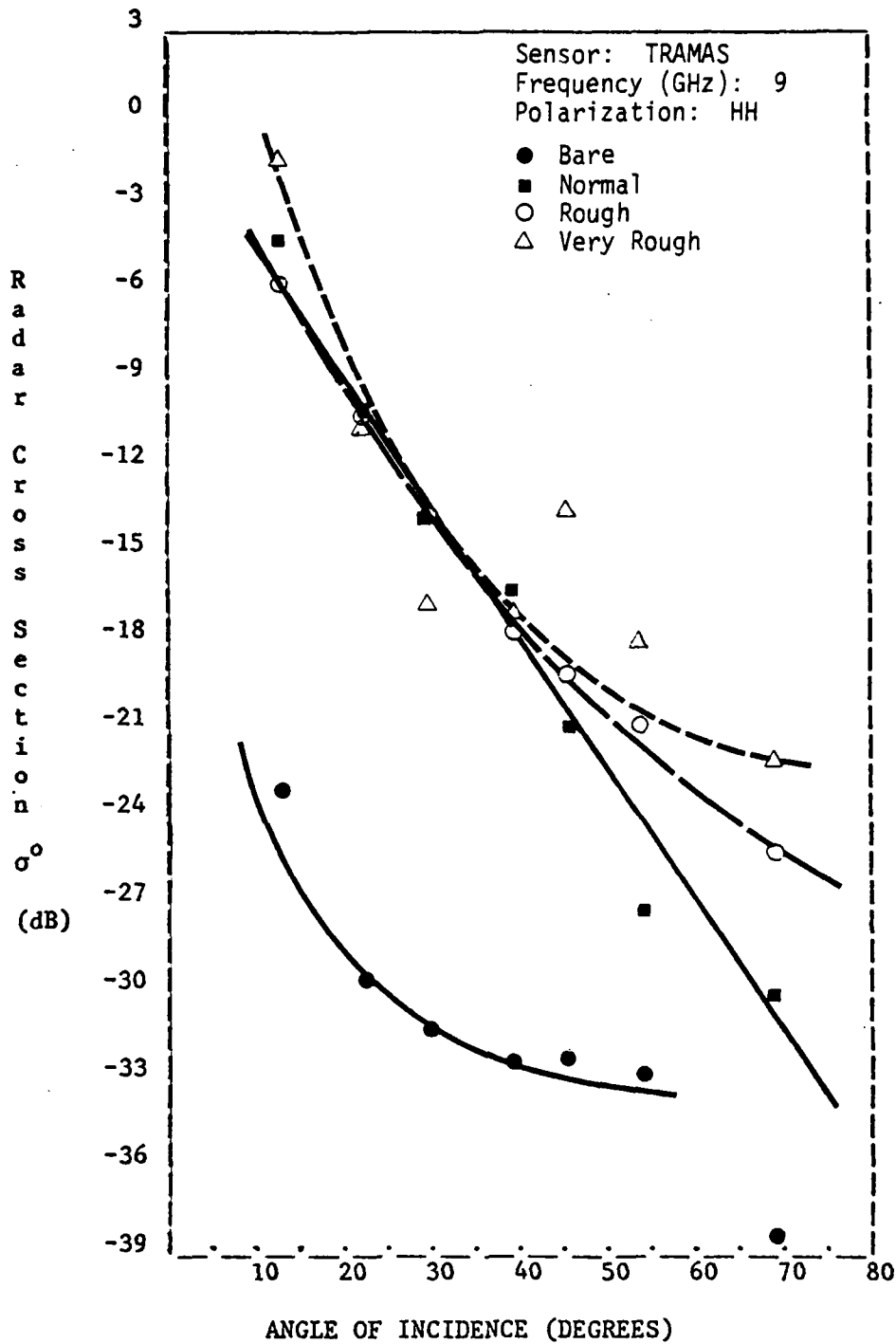


Figure 3.12. Scattering coefficient of Lake Ice with Bare, Normal, Rough, and Very Rough snow cover conditions at 9 GHz. (March 1979)

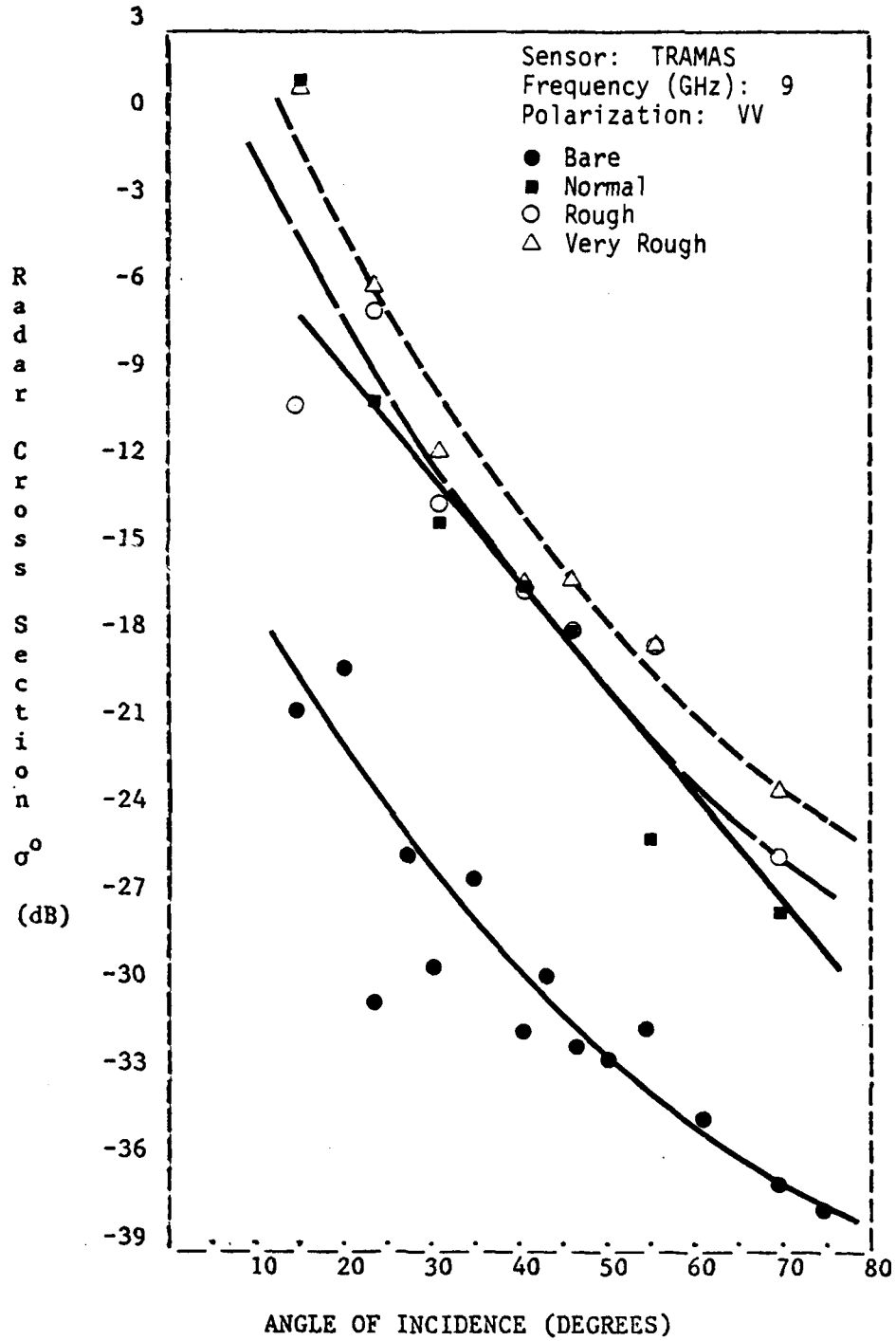


Figure 3.13. Scattering coefficient of Lake Ice with Bare, Normal, Rough, and Very Rough snow cover conditions at 9 GHz. (March 1979)

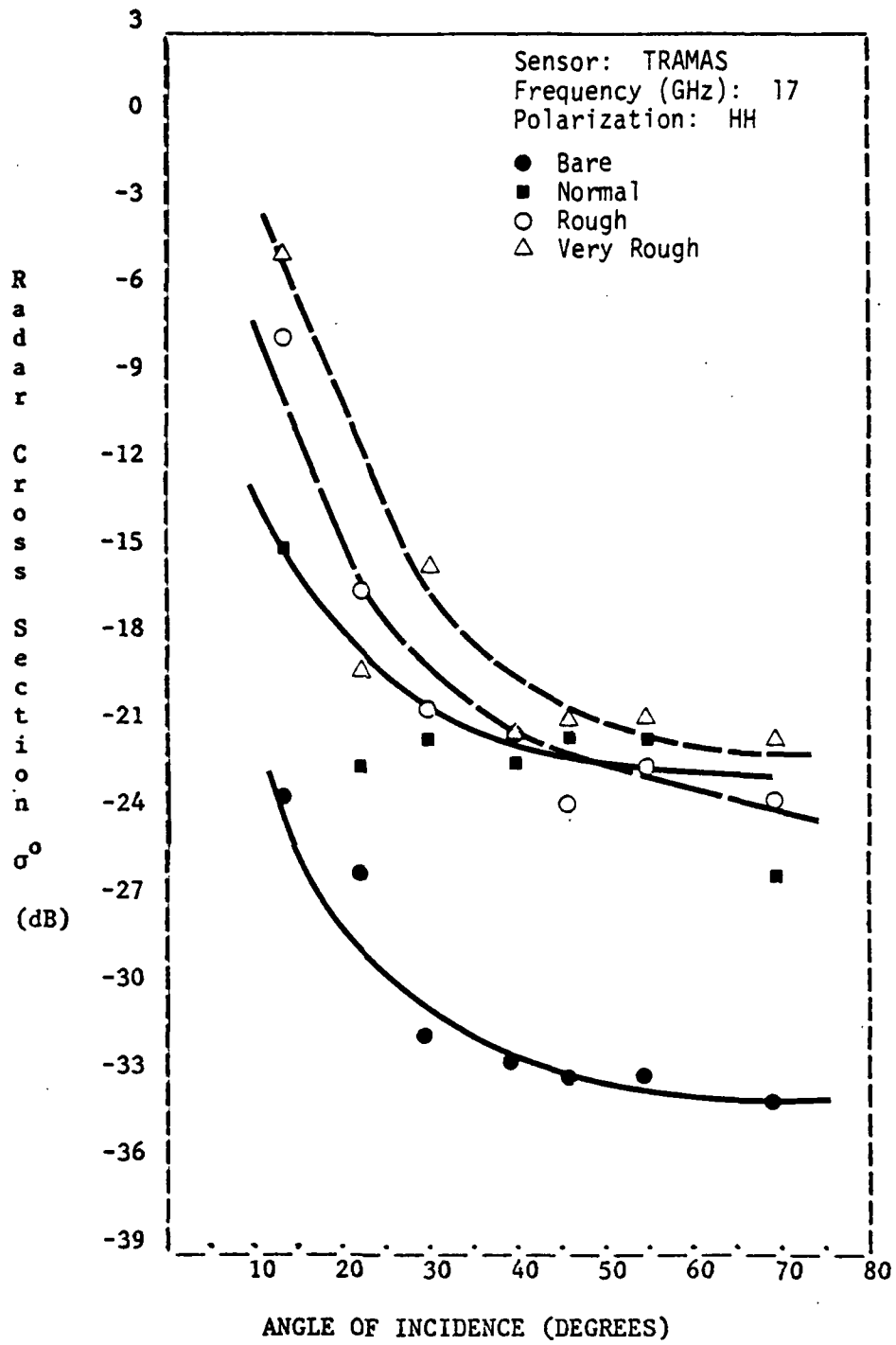


Figure 3.14. Scattering coefficient of Lake Ice with Bare, Normal, Rough, and Very Rough snow cover at 17 GHz. (March 1979)

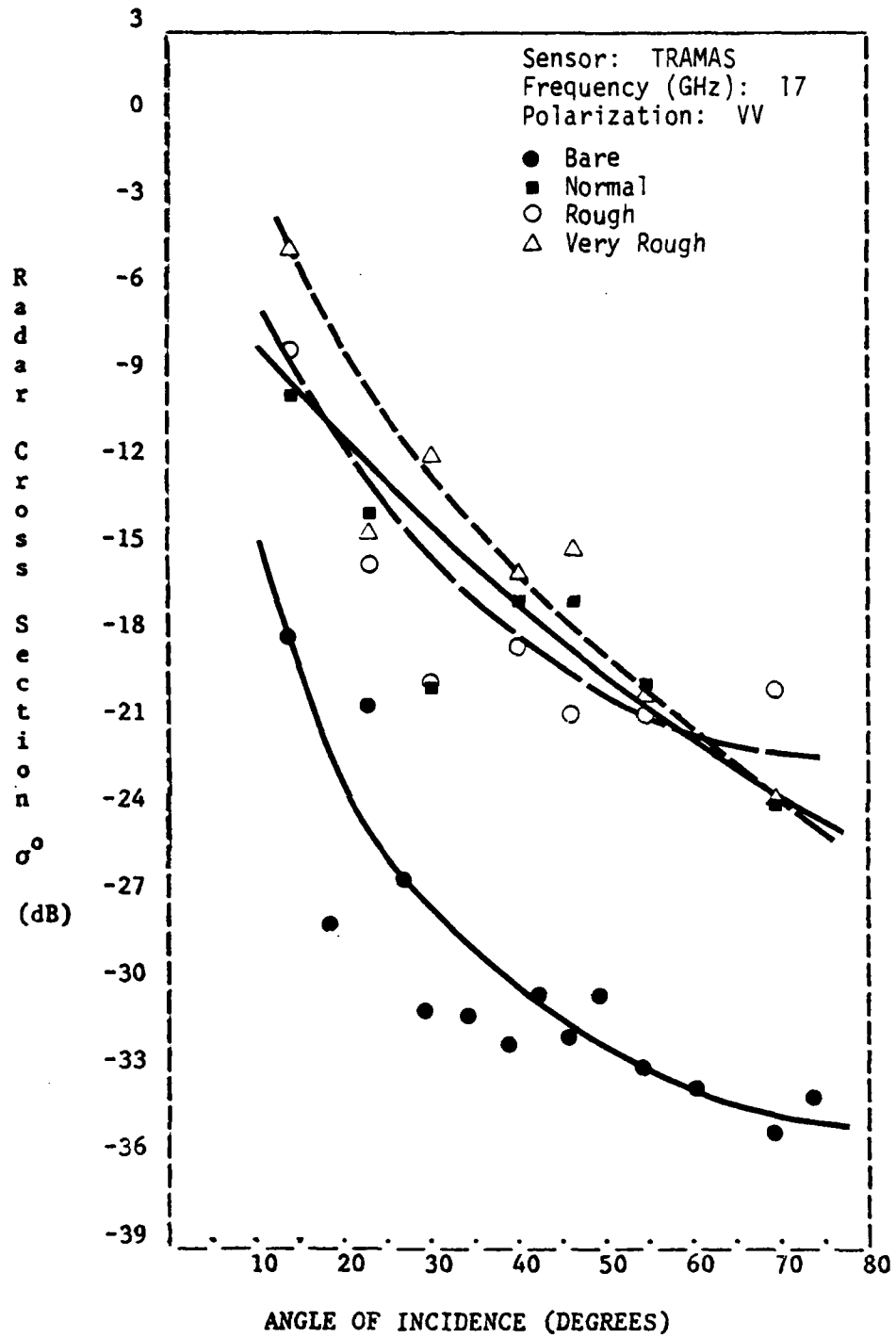


Figure 3.15. Scattering coefficient of Lake Ice with Bare, Normal, Rough, and Very Rough snow cover conditions at 17 GHz. (March 1979)

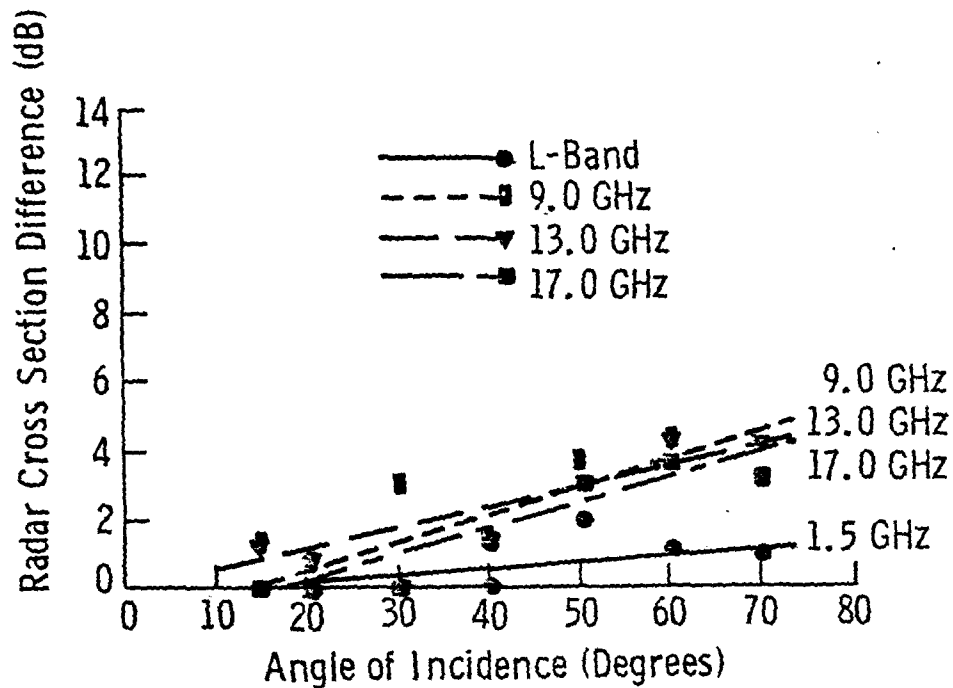


Figure 3.16 Difference Between Radar Cross-Section of Thin First-Year and Thick First-Year Sea Ice at 1.5, 9.0, 13.0, and 17.0 GHz with Vertical Polarization (TRAMAS, March 1979)

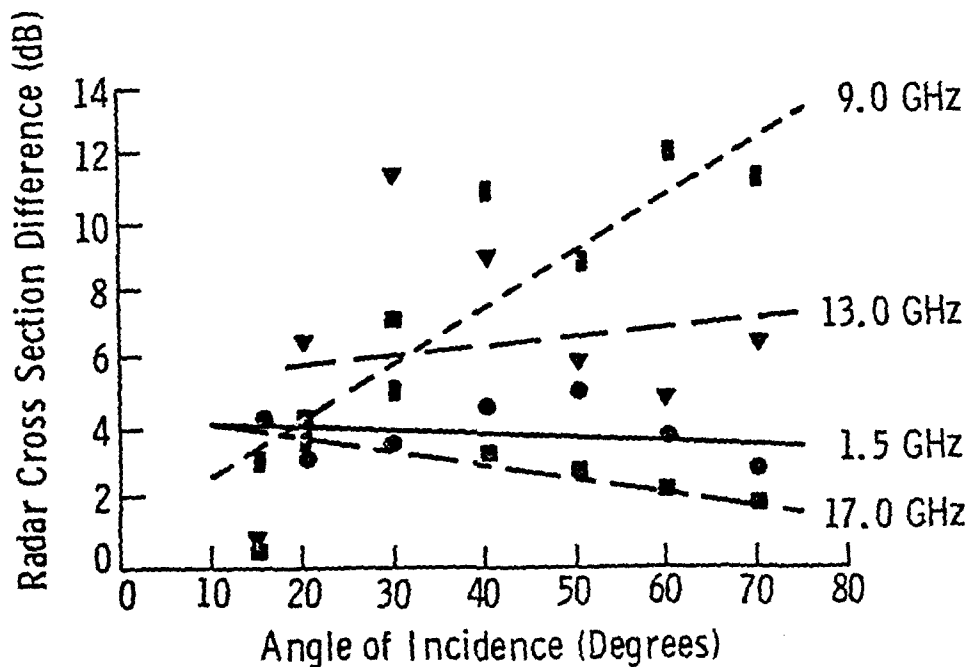


Figure 3.17 Difference Between Radar Cross-Section of Thick First-Year Sea Ice and Lake Ice at 1.5, 9.0, 13.0, and 17.0 GHz with Vertical Polarization (TRAMAS, March 1979)

#### 4.0 HELOSCAT RESULTS

The HELOSCAT system, although limited to VV polarization and only three angles of incidence, provides the opportunity to obtain many more samples from a large number of sites in much less time than is possible with the TRAMAS system. Figures 4.1 through 4.3 are graphs of the results from this phase of the experiment. The ordering of the ice types is consistent with the observations made for the TRAMAS phase of the experiment. Thin first-year scatter is higher than for thick first-year which is higher than for lake ice. At the lower frequencies brackish ice is very similar to thick first-year sea ice, but at 17 GHz the backscatter coefficient is 3 dB lower than the thick first-year sea ice scattering coefficient. The difference between thick first-year and thin first-year sea ice and between thick first-year sea ice and lake ice is plotted versus angle of incidence for 9, 13, and 17 GHz in Figures 4.4 and 4.5. The separation between thick and thin first-year sea ice is most prominent for the 9 GHz frequency and discrimination capability appears to be good for all angles of incidence between 10° and 70°. The range of separation in this case (2-6 dB) is larger than that observed with the TRAMAS system. This may be attributed to using different thin ice sites for the TRAMAS and HELOSCAT measurements. For lake ice the greatest difference occurs at 40° for a frequency of 17 GHz but all of the frequencies provide good discrimination capabilities for incidence angles between 10° and 60°. Overall, the angular response of the HELOSCAT data and the differences between ice types is consistent with the TRAMAS results.

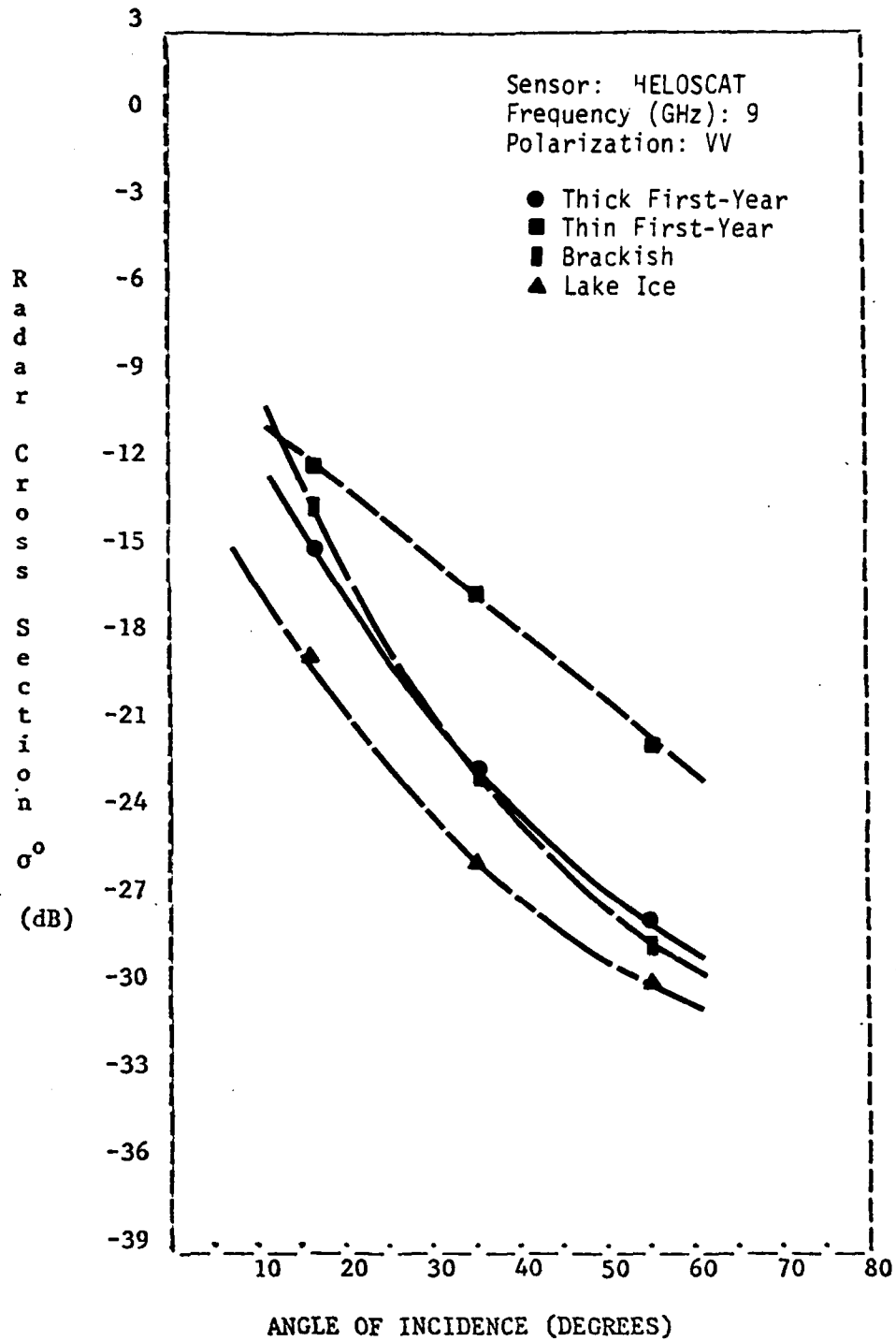


Figure 4.1 Average Scattering Coefficient of Thick First-Year, Thin First-Year, Brackish, and Lake Ice at 9 GHz. (March 1979)

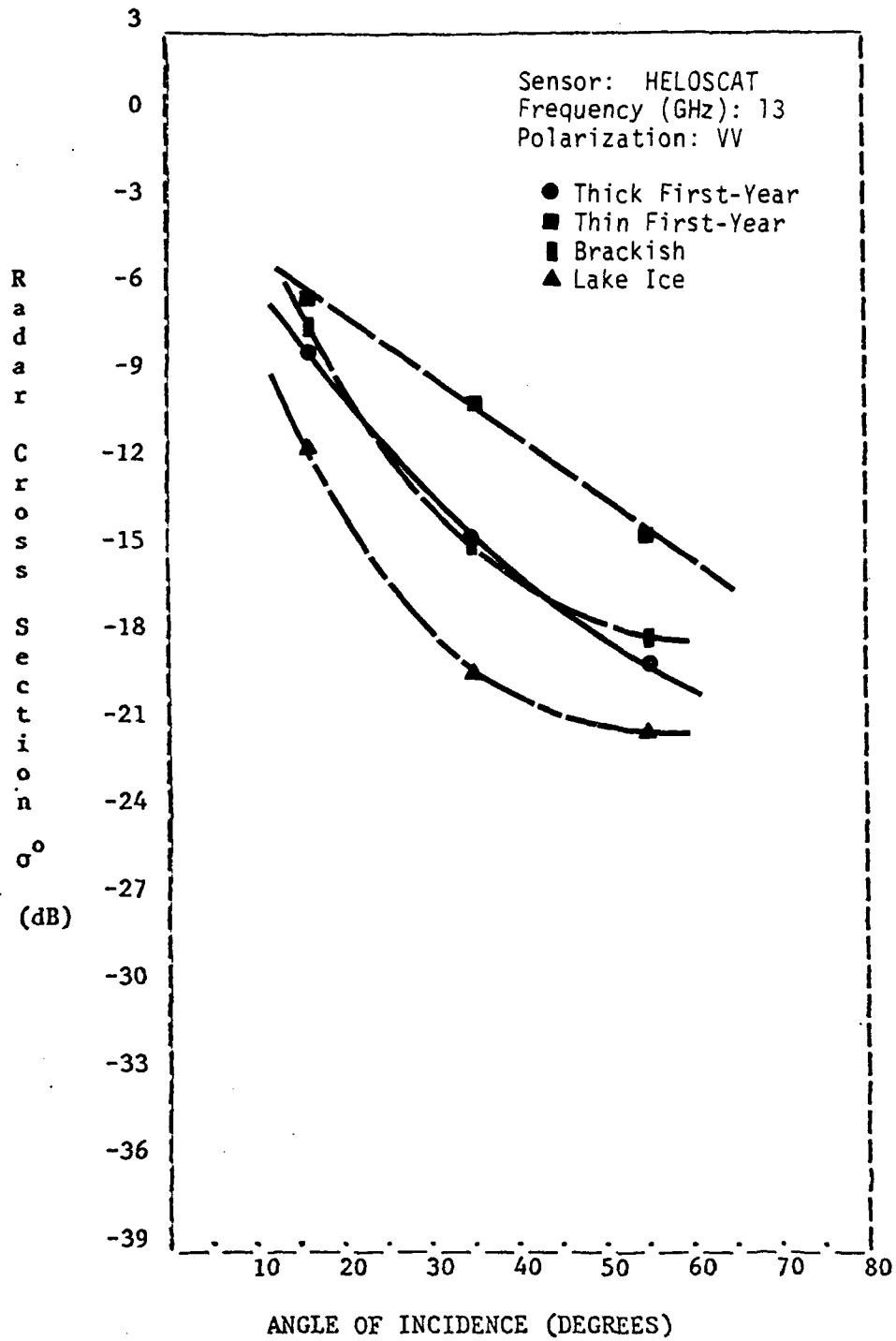


Figure 4.2 Average Scattering Coefficient of Thick First-Year, Thin First-Year, Brackish, and Lake Ice at 13 GHz. (March 1979)

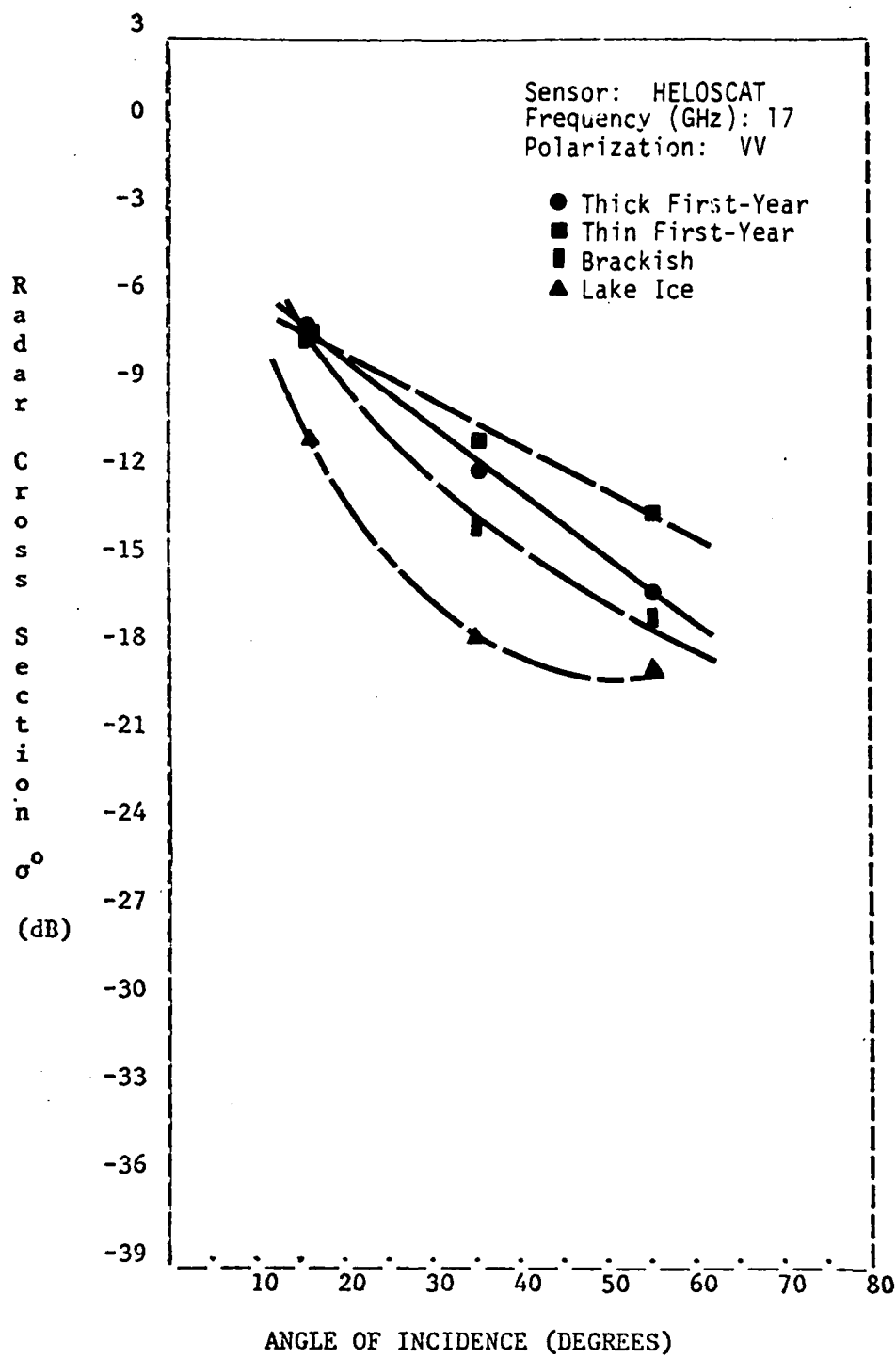


Figure 4.3 Average Scattering Coefficient of Thick First-Year, Thin First-Year, Brackish, and Lake Ice at 17 GHz. (March 1979).

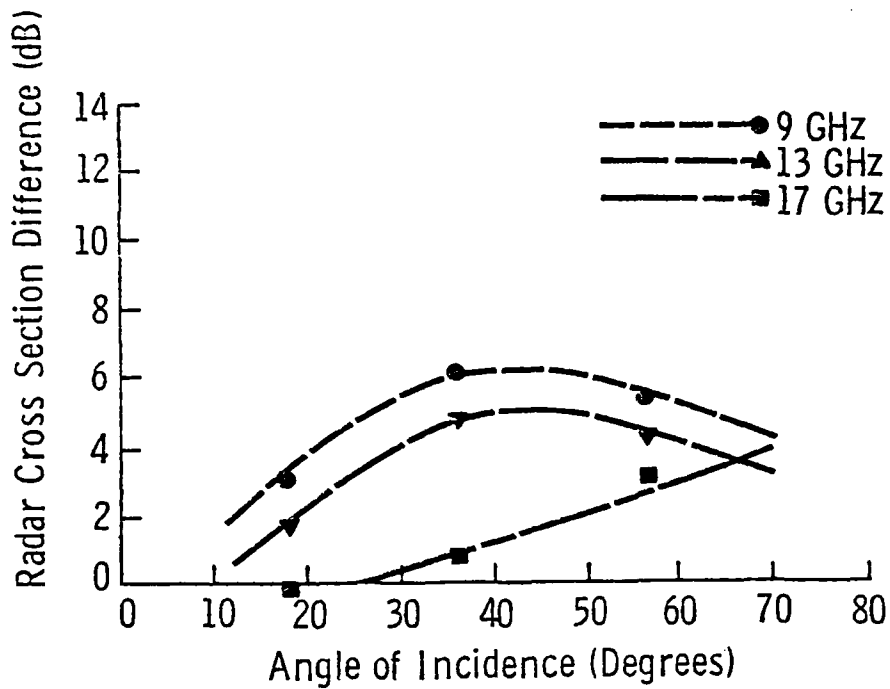


Figure 4.4 Difference Between Radar Cross-Section of Thin First-Year and Thick First-Year Sea Ice at 9.0, 13.0, and 17.0 GHz with Vertical Polarization (HELOSCAT, March 1979)

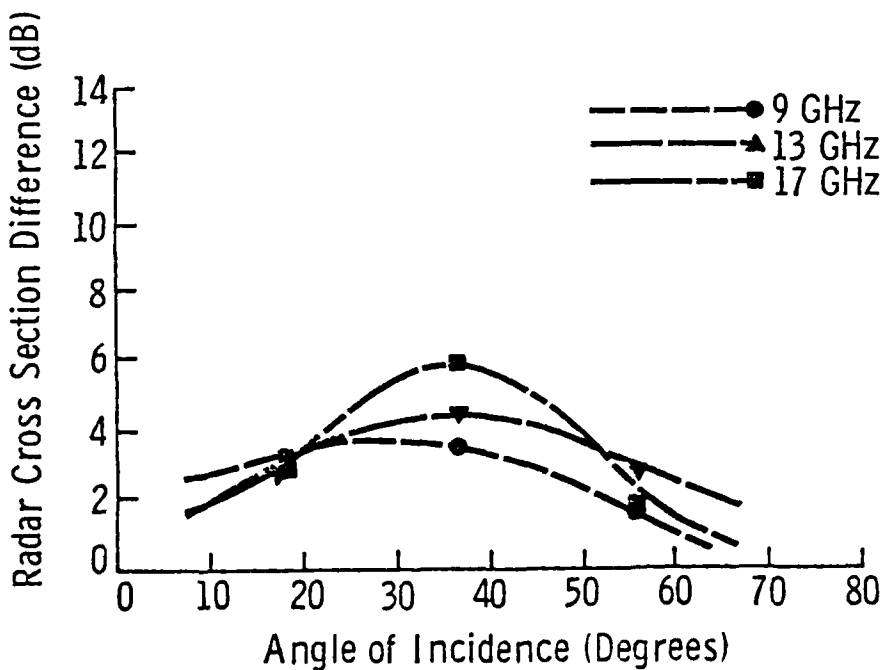


Figure 4.5 Difference Between Radar Cross-Section of Thick First-Year and Lake Ice at 9.0, 13.0, and 17.0 GHz with Vertical Polarization (HELOSCAT, March 1979)

## 5.0 FREQUENCY RESPONSE

Careful comparison of the TRAMAS and HELOSCAT data reveals that, although the angular response for each is very similar, the absolute magnitude for the different ice types varies with frequency. This is illustrated by comparing the frequency response of the data for the two systems (see Figures 5.1 and 5.2).

For the TRAMAS system lake ice demonstrates a linearly increasing trend while the thick and thin first-year sea ice both show parallel linearly decreasing trends versus frequency. Comparison of these results with those obtained in an earlier experiment [4] shows that the lake ice response is very similar to that of the prior data but the thick first-year sea ice response has changed from a positive to a negative slope. An analysis comparing the calibration from the two previous experiments with the March 1979 experiment indicates that the radar is operating consistently from year to year. For this reason, the change in slope must be related to some physical change in the ice conditions. Two major changes are available for consideration. The temperature during the 1979 experiment was much lower than the temperatures during the previous experiments. Since the lake ice response is consistent for all experiments it is not likely that temperature would be responsible for the major change observed for thick and thin first-year sea ice. Second, the sea ice studied during the 1979 experiment was pack ice while shorefast ice was studied in the previous experiments. Radar imagery of pack and shorefast first-year ice types indicates that there is a difference in the radar backscatter from the two and this may account for the different response.

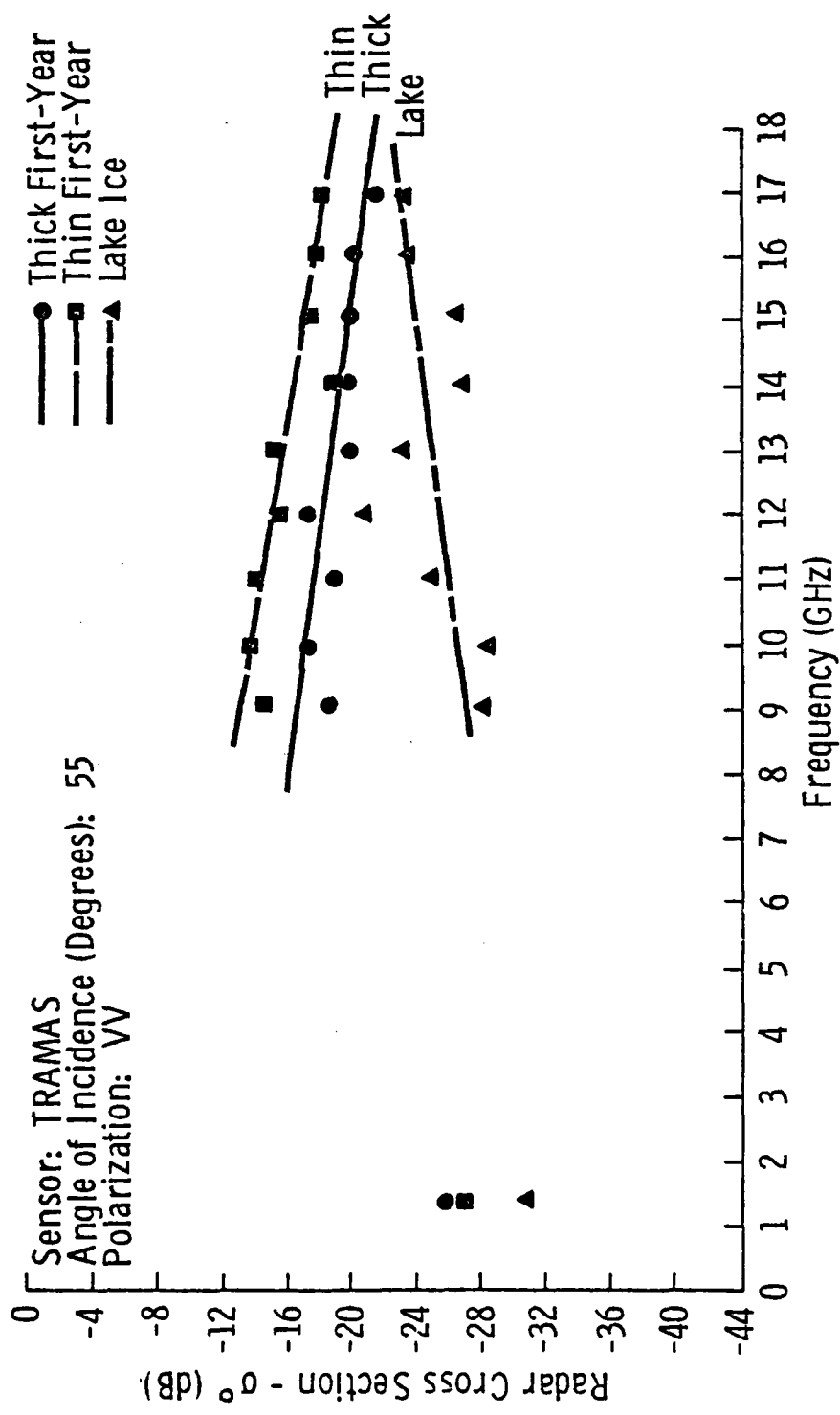


Figure 5.1 Scattering Coefficient Frequency Response of Thick First-Year, Thin First-Year, and Lake Ice (March 1979).

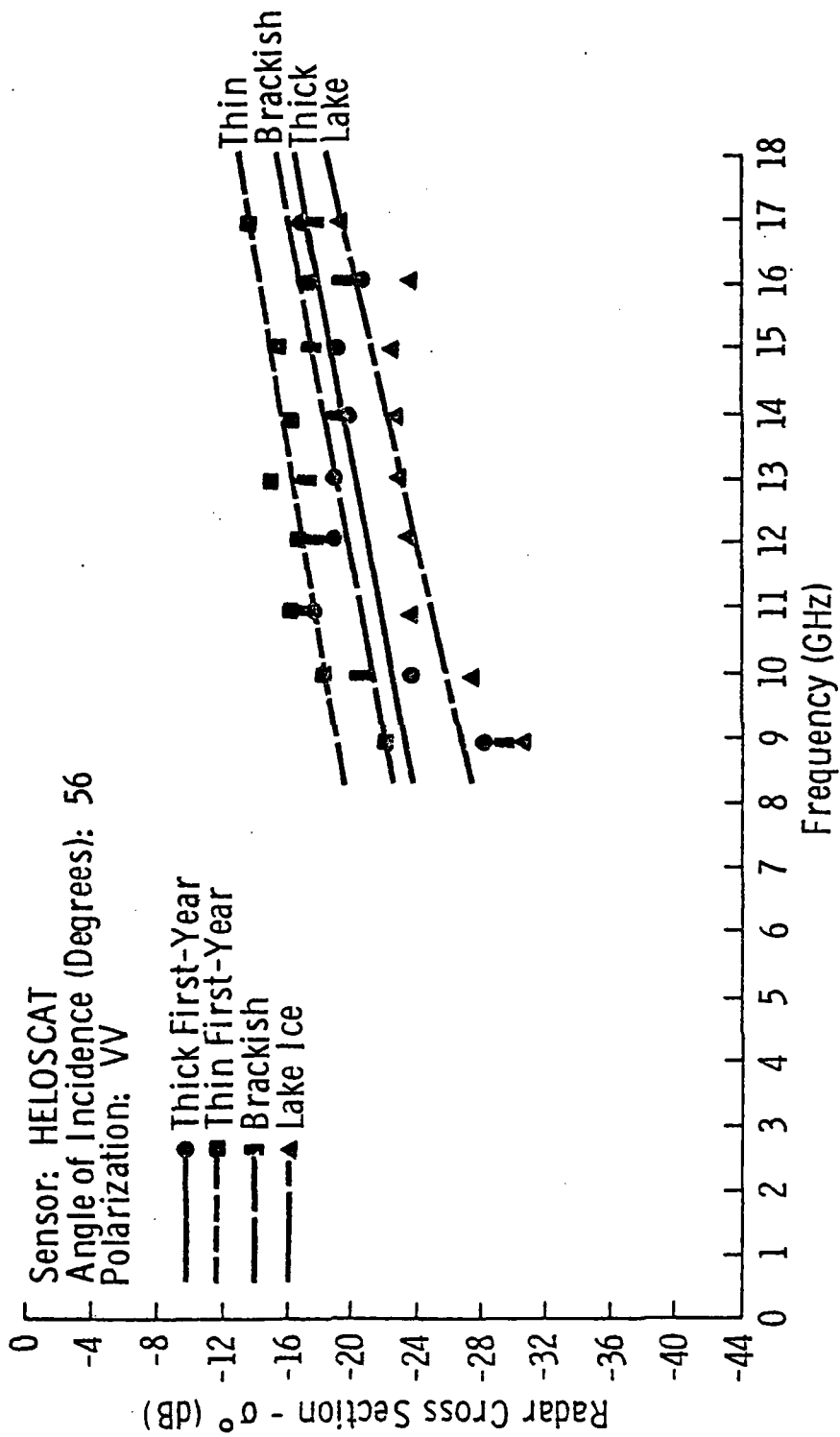


Figure 5.2 Scattering Coefficient Frequency Response of Thick First-Year, Thin First-Year, Brackish, and Lake Ice. (March 1979).

Linear regressions of the HELOSCAT data versus frequency indicate that all ice types have linearly increasing frequency responses. This is the cause of the magnitude differences observed for the TRAMAS and HELOSCAT results. The 9, 10, and 17 GHz frequencies are the most troublesome. If these points are neglected in the regression the frequency response begins to look very similar to that observed for the TRAMAS system. The most likely cause of this problem may be the calibration. The HELOSCAT system is calibrated on the ground by aiming the antennas horizontally at a Luneberg lens reflector supported on a stand at some fixed range. A preliminary calculation has shown that ground reflections during the calibration may interfere with the return from the lens. This interference may have a magnitude greater than 4 dB which would cause a significant change in the radar cross-section of the target. A more complete study of the HELOSCAT system calibration is scheduled for the near future.

## 6.0 CONCLUSIONS

The ability of radar to discriminate different types of ice has been well-demonstrated in this and previous experiments. The objective of the University of Kansas experiment program has been to obtain quantitative measurements of radar backscatter from ice which would help in the selection of the optimum combination of frequency, polarization, and angle of incidence for operational radar systems. To meet this objective, thick first-year sea ice, thin first-year sea ice, and fresh water lake ice were investigated at 1.5 and from 8-18 GHz, at angles of incidence from  $10^\circ$  to  $75^\circ$  (with respect to vertical), and with antenna transmit-receive polarizations of VV and VH for 1.5 GHz and VV, HV and HH for 8-18 GHz.

The L-band radar was found to have little ability to discriminate among the three ice types studied. At angles greater than  $40^\circ$  discrimination between thick first-year and thin first-year sea ice may be possible, especially at cross-polarization. The results of these experiments confirms what had been concluded from earlier SAR imagery. The practical use of L-band radar would be in topographical mapping.

The Ku-X-Band radar was able to discriminate among the ice types investigated. For angles of incidence greater than  $40^\circ$ , VV polarization and 9 GHz frequency appear to provide the best discrimination capability for all ice types investigated. A study of the effect of snow cover on the backscatter return from lake ice, also a part of this experiment, indicates that snow is a very important parameter which must be taken into account when making backscatter measurements. The difference in return from a surface with 4 cm of snow cover and a bare surface averaged 8 dB or more.

REFERENCES

- [1] Onstott, R.G., R.A. Hand, J.S. Patel, R.K. Moore, "Transportable Microwave Active Spectrometer 'TRAMAS' or 'MAS JR.', Design Memo," Remote Sensing Laboratory, Technical Memorandum TM 331-4, University of Kansas Center for Research, Inc., Lawrence, Kansas, September 1978.
- [2] Delker, C.V., R.G. Onstott, R.A. Hand, R.K. Moore, "Transportable Microwave Active Spectrometer 'TRAMAS' -- Modifications Report 1," Remote Sensing Laboratory, Technical Memorandum TM 331-5, University of Kansas Center for Research, Inc., Lawrence, Kansas, June 1979.
- [3] Delker, C.V., J.S. Patel, R.G. Onstott, "Installation Procedures for HELOSCAT Scatterometer on Bell Model 205," Remote Sensing Laboratory, Technical Memorandum TM 331-12, University of Kansas Center for Research, Inc., Lawrence, Kansas, May 1979.
- [4] Onstott, R.G., R.K. Moore, and W.F. Weeks, "Surface-Based Scatterometer Results of Arctic Sea Ice," IEEE Transactions on Geoscience Electronics, Vol. GE-17, No. 3, July 1979, pp. 78-85.